

Neutrino masses, dominant neutrinoless double beta decay, and observable lepton flavor violation in left-right models and SO(10) grand unification with low mass W_R, Z_R bosons

Ram Lal Awasthi,^δ M. K. Parida[†] and Sudhanwa Patra[†]

[†]Center of Excellence in Theoretical and Mathematical Sciences, Siksha 'O'Anusandhan University, Bhubaneswar-751030, India

^δHarish-Chandra Research Institute, Chhatnag Road, Jhusi, Allahabad 211019, India,
E-mails: ramlal@hri.res.in, paridamk@soauniversity.ac.in,
sudha.astro@gmail.com

ABSTRACT: While the detection of W_R -boson at the Large Hadron Collider is likely to resolve the mystery of parity violation in weak interaction, observation of neutrinoless double beta decay ($0\nu\beta\beta$) is expected to determine whether neutrinos are Majorana fermions. In this work we consider a class of LR models with TeV scale W_R, Z_R bosons but having parity restoration at high scales where they originate from well known Pati-Salam symmetry or $SO(10)$ grand unified theory minimally extended to accommodate inverse seesaw framework for neutrino masses. Most dominant new contribution to neutrinoless double beta decay is noted to occur via $W_L^- W_L^-$ mediation involving lighter sterile neutrino exchanges. The next dominant contribution is found to be through $W_L^- W_R^-$ mediation involving both light and heavy right-handed neutrino or sterile neutrino exchanges. The quark-lepton symmetric origin of the computed value of the Dirac neutrino mass matrix is also found to play a crucial role in determining these and other results on lepton flavor violating branching ratios for $\tau \rightarrow e + \gamma$, $\tau \rightarrow \mu + \gamma$, and $\mu \rightarrow e + \gamma$ accessible to ongoing search experiments. The underlying non-unitarity matrix is found to manifest in substantial CP-violating effects even when the leptonic Dirac phase $\delta_{CP} \simeq 0, \pi, 2\pi$. Finally we explore a possible origin of the model in non-supersymmetric $SO(10)$ grand unified theory where, in addition to low mass W_R^\pm and Z_R bosons accessible to Large Hadron Collider, the model is found to predict observable neutron-antineutron oscillation and lepto-quark gauge boson mediated rare kaon decay with $\text{Br}(K_L \rightarrow \mu \bar{e}) \simeq (10^{-9} - 10^{-11})$.

KEYWORDS: Beyond Standard Model, neutrino masses and mixing, neutrinoless double beta decay, Lepton Flavor Violation, Grand Unified Theory.

Contents

1. Introduction	2
2. Low scale left-right gauge theory and extended seesaw mechanism	4
2.1 The model	4
2.2 Neutrino masses and mixings	5
2.3 The unitarity violating matrix	6
2.4 Determination of μ_S from fits to neutrino oscillation data	9
3. Amplitudes for $0\nu\beta\beta$ decay and effective mass parameters	10
3.1 $W_L^- - W_L^-$ mediation	11
3.2 $W_R^- - W_R^-$ mediation	12
3.3 $W_L^- - W_R^-$ mediation	13
3.4 Doubly Charged Higgs contribution	14
3.5 Nuclear matrix elements and normalized effective mass parameters	14
4. Numerical estimation of effective mass parameters	16
4.1 Nearly standard contribution	16
4.2 Dominant non-standard contributions	17
5. Estimations on lepton flavor violating decays and J_{CP}	19
5.1 Branching ratio	20
5.2 CP-violation due to non-unitarity	21
6. Implementation in SO(10)	22
6.1 Symmetry breaking chain	23
6.2 Gauge coupling unification	24
6.3 Physical significance of mass scales	25
6.4 Importance of \mathcal{G}_{224D} intermediate symmetry	26
6.5 Determination of Dirac neutrino mass matrix	26
6.6 Suppressed induced contribution to $\nu - S$ mixing	35
7. Summary and Conclusion	36
A. APPENDIX	37
A.1 Block diagonalization and determination of \mathcal{M}_{BD}	38
A.1.1 Determination of \mathcal{W}_1	38
A.1.2 Determination of \mathcal{W}_2	39
A.2 Complete diagonalization and physical neutrino masses	40

1. Introduction

The Standard Model (SM) of strong, weak, and electromagnetic interactions has successfully confronted numerous experimental tests, yet its failures are exposed in neutrino masses and mixings, dark matter, dark energy, and baryon asymmetry of the universe. Apart from having a number of unknown parameters, the model does not explain why parity violation is monopoly of weak interaction. The suggestion of the origin of parity restoration is almost as old as the suggestion of parity violation itself when Lee and Yang [1] conjectured all basic interactions to be left-right symmetric. Subsequently, two classes of theories have been proposed to achieve the desired goal: (a) mirror symmetric extension of the Standard Model [2], (b) proposal of left-right symmetric gauge theory based upon $SU(2)_L \times SU(2)_R \times SU(4)_C$ ($\equiv \mathcal{G}_{224D}$) [3] and $SU(2)_L \times SU(2)_R \times U(1)_{B-L} \times SU(3)_C$ ($\equiv \mathcal{G}_{2213D}$) [4] with $g_{2L} = g_{2R}$. The minimal rank 5 grand unified theory (GUT) like $SO(10)$ [5] contains G_{224D} and G_{2213D} as its subgroups. The canonical (\equiv type-I) and type-II seesaw mechanisms [6–9] explaining tiny left-handed (LH) neutrino masses emerge naturally from $SO(10)$, G_{224D} , and G_{2213D} gauge theories provided both left-handed (LH) and right-handed (RH) neutrinos are Majorana fermions

$$m_\nu^I = -M_D \frac{1}{M_N} M_D^T, \quad m_\nu^{II} = f v_L, \quad (1.1)$$

where m_ν^I (m_ν^{II}) is the type-I (type-II) prediction of light LH neutrino mass matrix, M_D (M_N) is the Dirac (right-handed Majorana) neutrino mass. Here

$$v_L \simeq \beta v_{\text{wk}}^2 / M_{\Delta_L}, \quad (1.2)$$

β is a Higgs quartic coupling, v_{wk} is the electroweak VEV, and M_{Δ_L} is the left-handed triplet Higgs mass. Currently a number of dedicated experiments on neutrinoless double beta ($0\nu\beta\beta$) decay are in progress [10] while Heidelberg-Moscow experiment [11] has already claimed to have measured the effective mass parameter $M_{ee}^{\text{eff}} \simeq (0.23 - 0.56)$ eV and this observation might be hinting towards the Majorana nature of the light neutrinos [12].

$SO(10)$ GUT has the advantage of unifying the three basic forces (excluding gravity) and all fermions of the SM plus the RH neutrinos are unified into its single spinorial representation **16**. In view of the underlying quark-lepton symmetry \mathcal{G}_{224D} [3] of $SO(10)$, the Dirac neutrino mass matrix M_D could be similar to the up-quark mass matrix M_u in these theories, although \mathcal{G}_{2213D} [4] has also the alternative possibility of M_D to be similar to the charged lepton mass matrix M_ℓ if the symmetry does not emerge from \mathcal{G}_{224D} or $SO(10)$. In any case, if M_D is similar to the up-quark mass matrix or the charged lepton mass matrix, tiny neutrino masses uncovered by the neutrino oscillation experiments [13] push the seesaw

scales to be $> 10^{10}$ GeV rendering both the seesaw mechanisms to be inaccessible for direct experimental tests. In the process, the large scale of the associated RH gauge bosons (W_R^\pm, Z_R) prevent any visible nonstandard impact on weak interaction phenomenology including $0\nu\beta\beta$ decay [9] while throwing out the origin of left-right symmetric theory out of the arena of direct experimental tests at Large Hadron Collider (LHC) and other high energy accelerators in foreseeable future.

In attempts to conventional TeV scale parity-conserving left-right symmetric (LRS) model, it has been shown how type-II seesaw formula could be applied for light neutrino masses and mixings [14, 15] and how dominant contribution to neutrino-less double beta decay emerges in the $W_R^- - W_R^-$ mediated channel. It is expected that this theory could be verified by the Large Hadron Collider and other low energy experiments within the next few years.

In this work we show how in a different class of LR models [17] originating from high scale parity restoring Pati-Salam symmetry or $SO(10)$ grand unification, TeV scale W_R, Z_R bosons accessible to LHC are predicted. The Pati-Salam symmetry or $SO(10)$ grand unified theory each are minimally extended with one singlet fermion per generation to accommodate the experimentally verifiable gauged inverse seesaw frame work for neutrino masses [29–31]. Exploiting the other attractive aspect of such quark-lepton unified theories to represent fermion masses, we obtain the Dirac neutrino mass matrix as a natural prediction from the GUT-scale fit to all charged fermion masses. The type-I seesaw contribution to neutrino mass cancels out [19, 20] and the type-II seesaw contribution and another induced contribution are shown to be subdominant. As a result, the experimentally testable gauged inverse seesaw mechanism [19, 20] governs the light neutrino masses. The TeV scale masses of W_R^\pm and Z_R gauge bosons, and RH neutrinos are also directly accessible to accelerator tests [21–25].

For the first time we show that this model originating from high scale quark-lepton symmetry, gives quite dominant new contributions to $0\nu\beta\beta$ rate through the $W_L - W_L$ mediation via relatively light sterile neutrino exchange. The next dominant contribution is found to occur through the $W_L^- - W_R^-$ mediation with exchanges of light LH and heavy RH neutrinos or sterile neutrinos. The model also gives substantial non-unitarity effects and lepton flavor violating (LFV) decays accessible to ongoing experimental searches for $\tau \rightarrow e + \gamma$, $\tau \rightarrow \mu + \gamma$, and $\mu \rightarrow e + \gamma$. Both the Dirac neutrino mass matrix and the sterile neutrino masses are found to play significant roles in enhancing the $0\nu\beta\beta$ rates in the $W_L - W_L$ channel, LFV decay branching ratios, and new contributions to CP-violation due to non-unitarity effects.

Consistent with current PDG [33] values of precision data on electroweak mixing angle ($\sin^2\theta_W(M_Z)$), the QCD coupling constant ($\alpha_S(M_Z)$), and the electromagnetic fine-structure constant ($\alpha(M_Z)$), while the $SO(10)$ embedding of the conventional TeV scale parity-conserving LRS model has not been possible so far, we show how the present LR asymmetric gauge theory near the TeV scale with $g_{2L} \neq g_{2R}$ emerges from a non-supersymmetric (non-SUSY) grand unification framework like $SO(10)$ or high scale Pati-Salam symmetry. These two grand unified theories also predict observable neutron-antineutron oscillation [26] and rare kaon decay with $\text{Br}(K_L \rightarrow \mu \bar{e}) \simeq (10^{-9} - 10^{-11})$ [27] mediated

by lepto-quark gauge boson of $SU(4)_C$, although proton lifetime is found to be beyond the accessible limit of ongoing experiments. The derivation of the Dirac neutrino mass matrix used in all relevant computations is explicitly discussed in the context of high scale Pati-Salam symmetry or $SO(10)$ grand unification.

The plan of this paper is organized as follows: in Sec. 2 we briefly discuss the TeV scale left-right gauge theory with low-mass W_R, Z_R bosons, light neutrino masses and associated non-unitarity effects; in Sec. 3, we present various Feynman amplitudes for neutrinoless double beta decay; in Sec. 4, we give a detailed discussion for standard and non-standard contributions to the effective mass parameter for $0\nu 2\beta$ decay rate and in Sec. 5, we have discussed the branching ratios for lepton flavor violating decays. In Sec. 6, we implement the idea in a $SO(10)$ grand unified theory and derive Dirac neutrino mass matrix at the TeV scale. In Sec. 7 we summarize and conclude our results.

2. Low scale left-right gauge theory and extended seesaw mechanism

2.1 The model

As in the case of extended seesaw mechanism in LR models [20,28], besides the standard 16-fermions per generation including the RH neutrino, , we add one additional sterile fermion singlet for each generation ($S_i, i = 1, 2, 3$). We start with parity conserving left-right symmetric gauge theory, \mathcal{G}_{224D} [3] or \mathcal{G}_{2213D} [4], with equal gauge couplings ($g_{2L} = g_{2R}$) at high scales. In the Higgs sector we need both LH and RH triplets (Δ_L, Δ_R) as well as the LH and RH doublets (χ_L, χ_R) in addition to the bidoublet (Φ) and a D-parity odd singlet σ [17]. Their transformation properties under $\mathcal{G}_{224D} \supset \mathcal{G}_{2213D}$ are

$$\begin{aligned}
\Delta_L(3, 1, 10) &\supset \Delta_L(3, 1, -2, 1), \quad \Delta_R(1, 3, \overline{10}) \supset \Delta_R(1, 3, -2, 1), \\
\chi_L(2, 1, 4) &\supset \chi_L(2, 1, -1, 1), \quad \chi_R(2, 1, \overline{4}) \supset \chi_R(1, 2, -1, 1) \\
\sigma(1, 1, 1) &\supset \sigma(1, 1, 0, 1) \\
\Phi(2, 2, 1) &\supset \Phi(2, 2, 0, 1).
\end{aligned} \tag{2.1}$$

When the D-parity odd singlet σ acquires a VEV $\langle \sigma \rangle \sim M_P$, the LR discrete symmetry is spontaneously broken but the gauge symmetry G_{2213} remains unbroken leading to $M_{\Delta_R}^2 = (M_\Delta^2 - \lambda_\Delta \langle \sigma \rangle M')$, $M_{\chi_R}^2 = (M_\chi^2 - \lambda_\chi \langle \sigma \rangle M')$, where $\lambda_\Delta, \lambda_\chi$ are trilinear couplings and $\langle \sigma \rangle, M', M_\Delta, M_\chi$ are all $\sim \mathcal{O}(M_P)$, the RH Higgs scalar masses are made lighter depending upon the degree of fine tuning in λ_Δ and λ_χ . The asymmetry in the Higgs sector causes asymmetry in the $SU(2)_L$ and $SU(2)_R$ gauge couplings with $g_{2L}(\mu) > g_{2R}(\mu)$ for $\mu < M_P$. If one wishes to have W_R, Z_R mass predictions at nearly the same scales and generate Majorana neutrino masses, it is customary to break $G_{2213} \rightarrow \text{SM}$ by the VEV of the right handed triplet $\langle \Delta_R^0 \rangle \sim v_R$. We rather suggest a more appealing phenomenological scenario with $M_{W_R} > M_{Z_R}$ for which two step breaking of the asymmetric gauge theory to the SM is preferable : $G_{2213} \xrightarrow{M_R^+} G_{2113} \xrightarrow{M_R^0} \text{SM}$, where the first step of breaking that generates massive W_R^\pm bosons is implemented through the VEV of the heavier triplet $\Sigma_R(1, 3, 0, 1)$ carrying $B - L = 0$ and the second step of breaking is carried out by $\langle \Delta_R^0 \rangle \sim v_R$. At this

stage the RH neutral gauge boson gets mass which is kept closer to the current experimental lower bound $M_{Z'} \geq 1.162$ TeV for its visibility by high energy accelerators. We further gauge the extended seesaw mechanism at the TeV scale for which the VEV of the RH-doublet $\langle \chi_R^0 \rangle = v_\chi$ provides the $N - S$ mixing. The G_{2113} symmetric low-scale Yukawa Lagrangian is

$$\begin{aligned} \mathcal{L}_{\text{Yuk}} = & Y^\ell \bar{\psi}_L \psi_R \Phi + f \psi_R^c \psi_R \Delta_R + F \bar{\psi}_R S \chi_R \\ & + S^T \mu_S S + \text{h.c.} \end{aligned} \quad (2.2)$$

which gives rise to the 9×9 neutral fermion mass matrix after electroweak symmetry breaking

$$\mathcal{M} = \begin{pmatrix} 0 & 0 & M_D \\ 0 & \mu_S & M \\ M_D^T & M^T & M_N \end{pmatrix}, \quad (2.3)$$

where $M_D = Y \langle \Phi \rangle$, $M_N = f v_R$, $M = F \langle \chi_R^0 \rangle$. It is well known that the mass matrix M_D is determined from high scale symmetry and fits to charge fermion masses. In principle the $N - S$ mixing mass matrix M can assume any 3×3 , but for the sake of simplicity and economy of parameters we have found that the relevant model predictions are possible even if we choose it to have diagonal structure. In this case the three diagonal elements can be constrained by the existing experimental bound on a unitarity violating parameter. We have also utilized a predicted diagonal structure for M_N as well as other diagonal and general forms consistent with the $SO(10)$ GUT model.

2.2 Neutrino masses and mixings

In this model the RH neutrinos being heavier than the other mass scales with $M_N > M \gg M_D, \mu_S$ are at first integrated out from the Lagrangian leading to [19]

$$\begin{aligned} -\mathcal{L}_{\text{eff}} = & \left(M_D \frac{1}{M_N} M_D^T \right)_{\alpha\beta} \nu_\alpha^T \nu_\beta + \left(M_D \frac{1}{M_N} M^T \right)_{\alpha m} (\bar{\nu}_\alpha S_m + \bar{S}_m \nu_\alpha) \\ & + \left(M \frac{1}{M_N} M^T \right)_{mn} S_m^T S_n - \mu_S S_m^T S_n, \end{aligned} \quad (2.4)$$

which, in the (ν, S) basis, gives the 6×6 mass matrix

$$\mathcal{M}_{\text{eff}} = - \begin{pmatrix} M_D M_N^{-1} M_D^T & M_D M_N^{-1} M^T \\ M M_N^{-1} M_D^T & M M_N^{-1} M^T - \mu_S \end{pmatrix}, \quad (2.5)$$

while the 3×3 heavy RH neutrino mass matrix M_N is the other part of the full 9×9 neutrino mass matrix. This 9×9 mass matrix $\tilde{\mathcal{M}}_{\text{BD}}$ which results from the first step of block diagonalization procedure as discussed above and in the Appendix A is

$$\mathcal{W}_1^\dagger \mathcal{M}_\nu \mathcal{W}_1^* = \tilde{\mathcal{M}}_{\text{BD}} = \begin{pmatrix} \mathcal{M}_{\text{eff}} & 0 \\ 0 & M_N \end{pmatrix}, \quad (2.6)$$

where \mathcal{W}_1 has been derived as shown in eqn. (A.10) of Appendix A.

After the second step of block diagonalization, the type-I seesaw contribution cancels out and gives in the (ν, S, N) basis

$$\mathcal{W}_2^\dagger \tilde{\mathcal{M}}_{\text{BD}} \mathcal{W}_2^* = \mathcal{M}_{\text{BD}} = \begin{pmatrix} m_\nu & 0 & 0 \\ 0 & m_S & 0 \\ 0 & 0 & m_N \end{pmatrix}, \quad (2.7)$$

where \mathcal{W}_2 has been derived in eqn. (A.20) of the appendix. In eqn. (2.7), the three 3×3 matrices are

$$m_\nu \sim M_D M^{-1} \mu_S (M_D M^{-1})^T \quad (2.8)$$

$$m_S \sim \mu_S - M M_N^{-1} M^T \quad (2.9)$$

$$m_N \sim M_N, \quad (2.10)$$

the first of these being the well known inverse seesaw formula [29, 30].

In the third step, m_ν , m_S , and m_N are further diagonalized by the respective unitary matrices to give their corresponding eigenvalues

$$\begin{aligned} U_\nu^\dagger m_\nu U_\nu^* &= \hat{m}_\nu = \text{diag}(m_{\nu_1}, m_{\nu_2}, m_{\nu_3}), \\ U_S^\dagger m_S U_S^* &= \hat{m}_S = \text{diag}(m_{S_1}, m_{S_2}, m_{S_3}), \\ U_N^\dagger m_N U_N^* &= \hat{m}_N = \text{diag}(m_{N_1}, m_{N_2}, m_{N_3}). \end{aligned} \quad (2.11)$$

The complete mixing matrix [28, 31] diagonalizing the above 9×9 neutrino mass matrix given in eqn. (2.3) turns out to be

$$\begin{aligned} \mathcal{V} &\equiv \begin{pmatrix} \mathcal{V}_{\alpha i}^{\nu\hat{\nu}} & \mathcal{V}_{\alpha j}^{\nu\hat{S}} & \mathcal{V}_{\alpha k}^{\nu\hat{N}} \\ \mathcal{V}_{\beta i}^{S\hat{\nu}} & \mathcal{V}_{\beta j}^{S\hat{S}} & \mathcal{V}_{\beta k}^{S\hat{N}} \\ \mathcal{V}_{\gamma i}^{N\hat{\nu}} & \mathcal{V}_{\gamma j}^{N\hat{S}} & \mathcal{V}_{\gamma k}^{N\hat{N}} \end{pmatrix} \\ &= \begin{pmatrix} (1 - \frac{1}{2} X X^\dagger) U_\nu & (X - \frac{1}{2} Z Y^\dagger) U_S & Z U_N \\ -X^\dagger U_\nu & (1 - \frac{1}{2} \{X^\dagger X + Y Y^\dagger\}) U_S & (Y - \frac{1}{2} X^\dagger Z) U_N \\ y^* X^\dagger U_\nu & -Y^\dagger U_S & (1 - \frac{1}{2} Y^\dagger Y) U_N \end{pmatrix}, \end{aligned} \quad (2.12)$$

as shown in the appendix. In eqn. (2.13) $X = M_D M^{-1}$, $Y = M M_N^{-1}$, $Z = M_D M_N^{-1}$, and $y = M^{-1} \mu_S$.

2.3 The unitarity violating matrix

In this subsection we discuss briefly how non-unitarity arises in the lepton sector and how existing bounds on lepton flavor violating processes impose upper bounds on all the elements of the 3×3 non-unitarity matrix η . We have shown in Sec. 6 how different forms of the 3×3 RH neutrino mass matrix M_N are allowed by the fermion mass fits at the GUT scale including a diagonal form with specific eigen values. These matrices have been used to estimate model predictions in Sec. 4–Sec. 6. Using the constrained diagonal form of M as mentioned above, the mass matrix μ_S is determined using the gauged inverse see-saw

formula and neutrino oscillation data provided that the Dirac neutrino mass matrix M_D is also known. The determination of M_D at the TeV scale, basically originating from high-scale quark-lepton symmetry G_{224D} or $SO(10)$ GUT, is carried out by predicting its value at the high scale from fits to the charged fermion masses of three generations and then running down to the lower scales using the corresponding renormalization group equations (RGEs) in the top-down approach. It is to be noted that for fits to the fermion masses at the GUT scale, their experimental values at low energies are transported to the GUT scale using RGEs and the bottom-up approach. This procedure has been carried out in Sec. 6.5 by successfully embedding the LR gauge theory in a suitable non-SUSY G_{224} and $SO(10)$ framework and the result is

$$M_D = \begin{pmatrix} 0.02274 & 0.09891 - 0.01603i & 0.1462 - 0.3859i \\ 0.09891 + 0.01603i & 0.6319 & 4.884 + 0.0003034i \\ 0.1462 + 0.3859i & 4.884 - 0.0003034i & 117.8 \end{pmatrix} \text{ GeV.} \quad (2.14)$$

This value of M_D will be utilized for all applications discussed subsequently in this work including the fit to the neutrino oscillation data through the inverse seesaw formula, predictions of effective mass parameters in $0\nu\beta\beta$, computation of non-unitarity and CP-violating effects, and LFV decay branching ratios.

Usually diagonalizing the light active Majorana neutrino mass matrix by the PMNS mixing matrix U_{PMNS} gives $U_{\text{PMNS}}^\dagger m_\nu U_{\text{PMNS}}^* = \hat{m}_\nu = \text{diag}(m_{\nu_1}, m_{\nu_2}, m_{\nu_3})$. But, in this extended seesaw scheme, diagonalization is done by a matrix $\mathcal{N} \equiv \mathcal{V}^{\nu\nu}$ which is a part of the full 9×9 mixing matrix $\mathcal{V}_{9 \times 9}$. Using $\eta = \frac{1}{2} X X^\dagger$ where $X = M_D/M$, this diagonalizing matrix is

$$\mathcal{N} \simeq (1 - \eta) U_{\text{PMNS}}. \quad (2.15)$$

Thus η is a measure of deviation from unitarity in the lepton sector on which there has been extensive investigations in different models [28, 36, 37, 39, 40]. Assuming M to be diagonal for the sake of simplicity, $M \equiv \text{diag}(M_1, M_2, M_3)$, gives $\eta_{\alpha\beta} = \frac{1}{2} \sum_k M_{D\alpha k} M_k^{-2} M_{D\beta k}^*$,

measure of non-unitarity	Expt. bound [39]	C1	C2	C3
$ \eta_{ee} $	2.0×10^{-3}	3.5×10^{-8}	2.7×10^{-7}	3.1×10^{-6}
$ \eta_{e\mu} $	3.5×10^{-5}	3.9×10^{-7}	3.4×10^{-6}	1.5×10^{-5}
$ \eta_{e\tau} $	8.0×10^{-3}	9.4×10^{-6}	2.8×10^{-5}	6.4×10^{-5}
$ \eta_{\mu\mu} $	8.0×10^{-4}	4.7×10^{-6}	2.3×10^{-5}	6.9×10^{-5}
$ \eta_{\mu\tau} $	5.1×10^{-3}	1.1×10^{-4}	2.2×10^{-4}	3.2×10^{-4}
$ \eta_{\tau\tau} $	2.7×10^{-3}	2.7×10^{-3}	2.7×10^{-3}	2.7×10^{-3}

Table 1: Experimental bounds of the non-unitarity matrix elements $|\eta_{\alpha\beta}|$ (column **C0**) and their predicted values for degenerate (column **C1**), partially-degenerate (column **C2**), and non-degenerate (column **C3**) values of $M = \text{diag}(M_1, M_2, M_3)$ as described in cases (a), (b) and (c), respectively, in the text.

but it can be written explicitly for the degenerate case ($M_1 = M_2 = M_3 = M_d$)

$$\eta = \frac{1 \text{ GeV}^2}{M_d^2(\text{GeV}^2)} \begin{pmatrix} 0.0904 & 0.3894 - 0.9476i & 8.8544 - 22.7730i \\ 0.3894 + 0.9476i & 12.1314 & 289.22 + 0.00005i \\ 8.8544 + 22.7730i & 289.22 - 0.00005i & 6950.43 \end{pmatrix}. \quad (2.16)$$

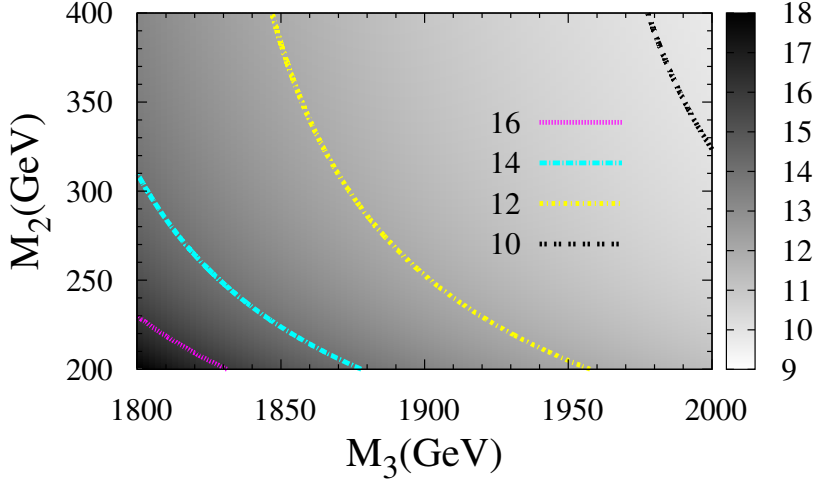


Figure 1: The contours of M_1 in the plane of M_2 and M_3 . The solid curves in the diagram represent M_3 dependence of M_2 for fixed values of M_1 using eqn. (2.17). The brightest top-right corner suggests that lightest M_1 may exist for largest values of M_2 and M_3 .

For the non-degenerate diagonal matrix M , saturating the experimental bound for $|\eta_{\tau\tau}| < 2.7 \times 10^{-3}$ [28, 37] gives

$$\frac{1}{2} \left[\frac{0.170293}{M_1^2} + \frac{23.8535}{M_2^2} + \frac{13876}{M_3^2} \right] = 2.7 \times 10^{-3}, \quad (2.17)$$

where the three numbers inside the square bracket are in GeV^2 . The correlation between M_2 and M_3 is shown in Fig. 1 where the allowed region in the brightest top right corner suggests the possibility of lightest M_1 for large values of M_2 and M_3 . It is clear from eq.(2.17) that M_i can not be arbitrary. Rather they are ordered with $M_3 > M_2 > M_1$ and also they are bounded from below with $M_1 > 5.6 \text{ GeV}$, $M_2 > 66.4 \text{ GeV}$, $M_3 > 1.6 \text{ TeV}$. In the degenerate case $M_1 = M_2 = M_3 = 1604.4 \text{ GeV}$. If we assume equal contribution to nonunitarity from all three terms in the left hand side of eq.(2.17), we get $M = \text{diag}(9.7, 115.1, 2776.6) \text{ GeV}$. Besides these constraints, we have used the primary criteria $M_N > M \gg M_D, \mu_S$ where $M_N \leq O(v_R)$, the G_{2113} breaking scale in choosing the elements of M .

The elements of η have been listed in the Table. 1 for (a) degenerate $M = \text{diag}(1604.4, 1604.4, 1604.4) \text{ GeV}$, (b) partially degenerate $M = \text{diag}(100, 100, 2151.58) \text{ GeV}$, and (c) non degenerate $M = \text{diag}(9.73, 115.12, 2776.6) \text{ GeV}$ in columns **C1**, **C2** and **C3**, respectively, where in column **C0**, experimental bounds are presented [39].

m_ν	M	μ_S
NH	(a)	$\begin{pmatrix} 9.457 + 4.114i & -2.073 - 0.904i & 0.087 - 0.001i \\ \cdot & 0.455 + 0.198i & -0.019 - 0.0003i \\ \cdot & \cdot & 0.00069 - 0.000027i \end{pmatrix} \text{ GeV}$
	(b)	$\begin{pmatrix} 0.037 + 0.016i & -0.008 - 0.003i & 0.007 - 0.0001i \\ \cdot & 0.001 + 0.0007i & -0.001 + 0.00002i \\ \cdot & \cdot & 0.001 - 0.0004i \end{pmatrix} \text{ GeV}$
	(c)	$\begin{pmatrix} 3.476 + 1.512i & -9.018 - 3.933i & 9.180 + 0.141i \\ \cdot & 23.410 + 10.230i & -23.840 - 0.385i \\ \cdot & \cdot & 20.670 - 8.246i \end{pmatrix} \times 10^{-4} \text{ GeV}$

Table 2: Structure of μ_S from neutrino oscillation data for normal-hierarchy (NH) of light neutrino masses, $m_\nu = (0.00127, 0.008838, 0.04978)$ eV and different mass pattern of M : (a) $M = (1604.442, 1604.442, 1604.442)$ GeV, (b) $M = (100.0, 100.0, 2151.5)$ GeV, and (c) $M = (9.72, 115.12, 2776.57)$ GeV.

2.4 Determination of μ_S from fits to neutrino oscillation data

We utilize the central values of parameters obtained from recent global fit to the neutrino oscillation data [41]

$$\begin{aligned}
\sin^2 \theta_{12} &= 0.320, & \sin^2 \theta_{23} &= 0.427, \\
\sin^2 \theta_{13} &= 0.0246, & \delta_{CP} &= 0.8\pi, \\
\Delta m_{\text{sol}}^2 &= 7.58 \times 10^{-5} \text{ eV}^2, \\
|\Delta m_{\text{atm}}|^2 &= 2.35 \times 10^{-3} \text{ eV}^2,
\end{aligned} \tag{2.18}$$

and ignore Majorana phases ($\alpha_1 = \alpha_2 = 0$). Then using the non-unitarity mixing matrix $\mathcal{N} = (1 - \eta) U_{\text{PMNS}}$ and the relation $m_\nu = \mathcal{N} \hat{m}_\nu \mathcal{N}^T$, we derive the μ_S matrix by inverting the inverse seesaw formula,

m_ν	M	μ_S
IH	(a)	$\begin{pmatrix} 82.04 + 2.261i & -17.75 - 0.508i & 0.642 - 0.251i \\ \cdot & 3.842 + 0.114i & -0.138 + 0.054i \\ \cdot & \cdot & 0.0042 - 0.0040i \end{pmatrix} \text{ GeV}$
	(b)	$\begin{pmatrix} 0.318 + 0.0088i & -0.0689 - 0.0019i & +0.0536 - 0.0209i \\ \cdot & +0.0149 + 0.00044i & -0.0116 - 0.0045i \\ \cdot & \cdot & 0.0075 - 0.0073i \end{pmatrix} \text{ GeV}$
	(c)	$\begin{pmatrix} 3.015 + 0.083i & -7.72 - 0.221i & 6.73 - 2.62i \\ \cdot & 19.78 + 0.58i & -17.25 + 6.714i \\ \cdot & \cdot & 12.41 - 12.08i \end{pmatrix} \times 10^{-3} \text{ GeV}$

Table 3: Same as Tab. 2 but for inverted-hierarchy (IH) of light neutrino masses $m_\nu = (0.04901, 0.04978, 0.00127)$ eV.

$$\begin{aligned}
\mu_S &= X^{-1} \mathcal{N} \hat{m}_\nu \mathcal{N}^T (X^T)^{-1} \\
&= \begin{pmatrix} 3.476 + 1.512i & -9.018 - 3.933i & 9.180 + 0.141i \\ \cdot & 23.410 + 10.230i & -23.840 - 0.385i \\ \cdot & \cdot & 20.670 - 8.246i \end{pmatrix} \times 10^{-4} \text{ GeV} \quad (2.19)
\end{aligned}$$

where we have used normal hierarchy (NH) for light neutrino masses, $\hat{m}_\nu = (0.00127, 0.00885, 0.0495)$ eV in the non degenerate case of $M = \text{diag}(9.72, 115.12, 2776.57)$ GeV. For the sake of completeness, we have presented few solutions of μ_S matrix for degenerate, partially-degenerate and non-degenerate values of M as shown in the Tables 2 and 3 corresponding to NH and IH light neutrino masses, respectively. For the quasi-degenerate (QD) pattern of light neutrino masses the matrix μ_S can be easily derived and all our analyses carried out in Sec. 3 - Sec.5 can be repeated.

3. Amplitudes for $0\nu\beta\beta$ decay and effective mass parameters

In this section we discuss analytically the contributions of various Feynman diagrams in $W_L^- - W_L^-$ channel (with two left-handed currents), $W_R^- - W_R^-$ channel (with two right-handed currents), and $W_L^- - W_R^-$ channel (with one left-handed and one right-handed current) and estimate the corresponding amplitudes in the TeV scale asymmetric left-right gauge theory with extended seesaw mechanism.

The charged current interaction Lagrangian for leptons in this model in the flavor basis is

$$\mathcal{L}_{\text{CC}} = \frac{g}{\sqrt{2}} \sum_{\alpha=e,\mu,\tau} \left[\bar{\ell}_{\alpha L} \gamma_\mu \nu_{\alpha L} W_L^\mu + \bar{\ell}_{\alpha R} \gamma_\mu N_{\alpha R} W_R^\mu \right] + \text{h.c.} \quad (3.1)$$

Following the masses and mixing for neutrinos in the extended seesaw scheme [28] discussed in Sec. 2, LH and RH neutrino flavor states are expressed in terms of mass eigenstates ($\hat{\nu}_i, \hat{S}_i, \hat{N}_i$)

$$\nu_{\alpha L} \sim \mathcal{V}_{\alpha i}^{\nu\nu} \hat{\nu}_i + \mathcal{V}_{\alpha i}^{\nu S} \hat{S}_i + \mathcal{V}_{\alpha i}^{\nu N} \hat{N}_i, \quad (3.2)$$

$$N_{\alpha R}^C \sim \mathcal{V}_{\alpha i}^{N\nu} \hat{\nu}_i + \mathcal{V}_{\alpha i}^{NS} \hat{S}_i + \mathcal{V}_{\alpha i}^{NN} \hat{N}_i. \quad (3.3)$$

In addition, there is a possibility where left-handed and right-handed gauge bosons mix with each other and, hence, the physical gauge bosons are linear combinations of W_L and W_R as

$$\begin{cases} W_1 = \cos \zeta_{\text{LR}} W_L + \sin \zeta_{\text{LR}} W_R \\ W_2 = -\sin \zeta_{\text{LR}} W_L + \cos \zeta_{\text{LR}} W_R \end{cases} \quad (3.4)$$

with

$$|\tan 2\zeta_{\text{LR}}| \sim \frac{v_u v_d}{v_R^2} \sim \frac{v_d g_{2R}^2}{v_u g_{2L}^2} \left(\frac{M_{W_L}^2}{M_{W_R}^2} \right) \leq 10^{-4}. \quad (3.5)$$

As it is evident from the charged-current interaction given in eqn.(3.1) and taking left- and right-handed gauge boson mixings into account given in eqn.(3.4), there can be several

Feynman diagrams which contribute to neutrinoless double beta decay transition in the TeV scale left-right gauge theory. They can be broadly classified as due to $W_L^- - W_L^-$ mediation purely due to two left-handed currents, $W_R^- - W_R^-$ mediation purely due to two right-handed currents, and $W_L^- - W_R^-$ mediations due to one left-handed current and one right-handed current which are denoted by LL, RR, and LR in the superscripts of the corresponding amplitudes. These diagrams are shown in Fig. 2 - Fig. 5.

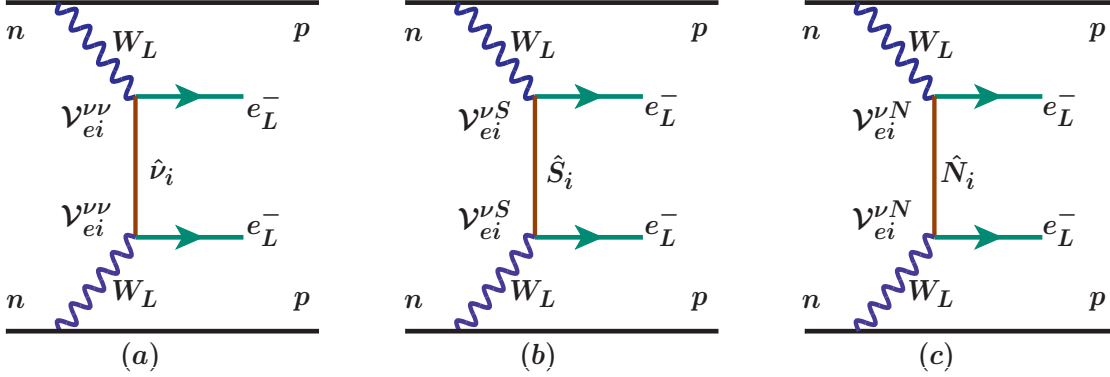


Figure 2: Feynman diagrams for neutrinoless double beta decay ($0\nu\beta\beta$) contribution with virtual Majorana neutrinos $\hat{\nu}_i$, \hat{S}_i , and \hat{N}_i along with the mediation of two W_L -bosons.

3.1 $W_L^- - W_L^-$ mediation

The most popular standard contribution is due to $W_L^- - W_L^-$ mediation by light neutrino exchanges. But one of our major contribution in this work is that even with $W_L^- - W_L^-$ mediation, the sterile neutrino exchange allowed within the extended seesaw mechanism of the model can yield much more dominant contribution to $0\nu\beta\beta$ decay rate than the standard one. With the exchange of left-handed light neutrinos ($\hat{\nu}_i$), sterile neutrinos (\hat{S}_j), and RH heavy Majorana neutrinos (\hat{N}_k), the diagrams shown in Fig. 2.(a), Fig. 2.(b), and Fig. 2.(c) contribute

$$\mathcal{A}_\nu^{LL} \propto \frac{1}{M_{W_L}^4} \sum_{i=1,2,3} \frac{(\mathcal{V}_{ei}^{\nu\nu})^2 m_{\nu_i}}{p^2}, \quad (3.6)$$

$$\mathcal{A}_S^{LL} \propto \frac{1}{M_{W_L}^4} \sum_{j=1,2,3} \frac{(\mathcal{V}_{ej}^{\nu S})^2}{m_{S_j}}, \quad (3.7)$$

$$\mathcal{A}_N^{LL} \propto \frac{1}{M_{W_L}^4} \sum_{k=1,2,3} \frac{(\mathcal{V}_{ek}^{\nu N})^2}{m_{N_k}}, \quad (3.8)$$

where $|p^2| \simeq (190 \text{ MeV})^2$ represents neutrino virtuality momentum [42].

To understand the origin and the role of the relevant Majorana mass insertion terms as source of $|\Delta L| = 2$ lepton number violation in the new contribution to $0\nu\beta\beta$ process, we briefly discuss the example of sterile fermion (S) exchange corresponding to Fig. 2.(b) and

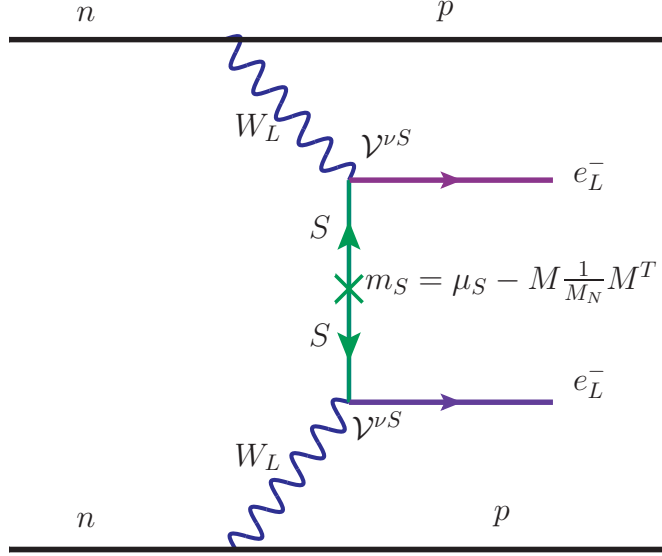


Figure 3: Feynman diagram for neutrinoless double beta decay contribution by $W_L^- - W_L^-$ mediation and by the exchange of virtual sterile neutrinos (S). The Majorana mass insertion has been shown explicitly by a cross.

Fig. 3. At first we note that, in contrast to the inverse seesaw framework with pseudo-Dirac type RH neutrinos [36,37] where the only source of $|\Delta L| = 2$ lepton number violation is μ_S , in the present case of extended seesaw the Majorana mass for S gets an additional dominant contribution $MM_N^{-1}M^T$ as shown explicitly in eq. (2.4) and eq. (2.9). The expanded form of the Feynman diagram with both the mass insertion terms is shown in Fig. 3 which gives

$$\mathcal{A}_S^{LL} \propto \frac{1}{M_{W_L}^4} P_L \left[\mathcal{V}^{\nu S} \frac{1}{\not{p} - m_S} m_S \frac{1}{\not{p} - m_S} \mathcal{V}^{\nu S^T} \right]_{ee} P_L, \quad (3.9)$$

where we have used $m_S = \mu_S - M M_N^{-1} M^T$. Within the model approximation and allowed values of parameters, $|m_S| \simeq |M M_N^{-1} M^T| \gg |p| \gg |\mu_S|$ resulting in

$$\mathcal{A}_S^{LL} \propto \frac{1}{M_{W_L}^4} \left[\mathcal{V}^{\nu S} \left(\frac{\mu_S}{m_S^2} + \frac{1}{m_S} \right) \mathcal{V}^{\nu S^T} \right]_{ee}, \quad (3.10)$$

where the first term is negligible compared to the second term, and we get eq. (3.7). On the other hand, in the case of pseudo-Dirac RH neutrinos corresponding to $M_N = 0$ in eq. (2.3), the only Majorana mass insertion term in Fig. 3 is through $m_S = \mu_S$ with $|\mu_S| \ll |p|$. Then eq. (3.9) gives $\mathcal{A}_S^{LL} \propto \frac{1}{M_{W_L}^4} \frac{(\mathcal{V}^{\nu S})^2 \mu_S}{p^2} \simeq \frac{1}{M_{W_L}^4} \frac{m_\nu}{p^2}$ which is similar to the standard contribution. This latter situation is never encountered in the parameter space of the present models.

3.2 $W_R^- - W_R^-$ mediation

This contribution arising purely out of right-handed weak currents can also occur by the exchanges of $\hat{\nu}_i$, \hat{S}_i , and \hat{N}_i and the corresponding diagrams are shown in Fig. 4.(a), Fig.

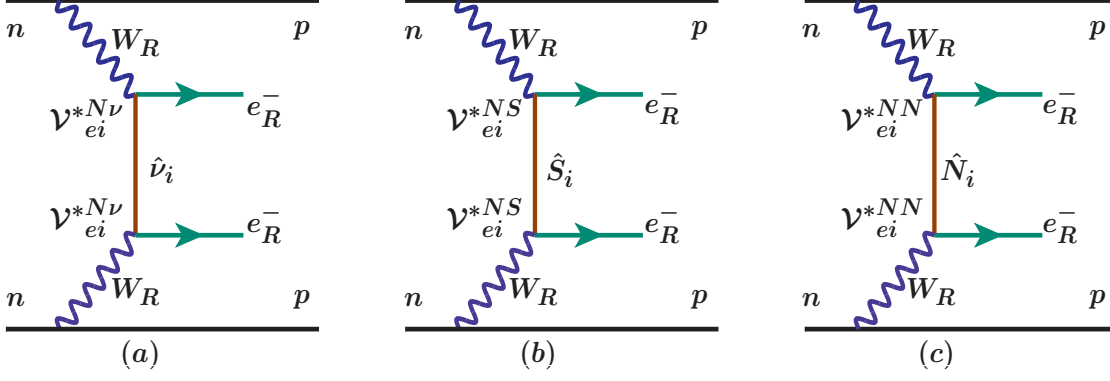


Figure 4: Same as Fig. 2 but with $W_R - W_R$ mediation.

4.(b), and Fig. 4.(c) leading to the amplitudes

$$\mathcal{A}_\nu^{RR} \propto \frac{1}{M_{W_R}^4} \frac{(\mathcal{V}_{ei}^{N\nu})^2 m_{\nu_i}}{p^2}, \quad (3.11)$$

$$\mathcal{A}_S^{RR} \propto \frac{1}{M_{W_R}^4} \frac{(\mathcal{V}_{ej}^{NS})^2}{m_{S_j}}, \quad (3.12)$$

$$\mathcal{A}_N^{RR} \propto \frac{1}{M_{W_R}^4} \frac{(\mathcal{V}_{ej}^{NN})^2}{m_{N_k}}. \quad (3.13)$$

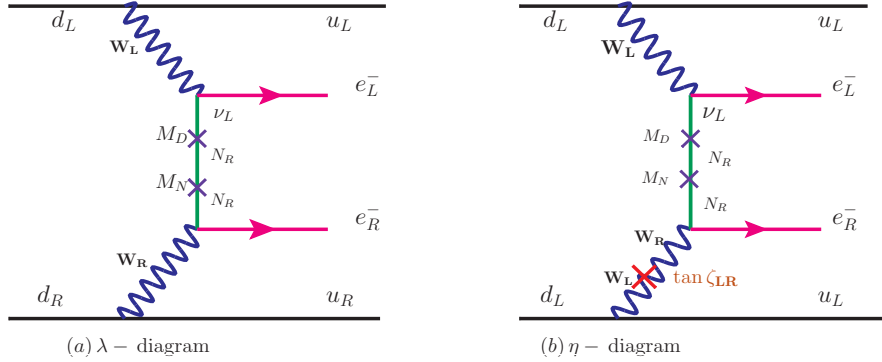


Figure 5: Mixed Feynman diagram with $W_L - W_R$ mediation; left-panel is for λ -mechanism and right-panel is for η -mechanism as defined in Ref. [44] and discussed in the text.

3.3 $W_L^- - W_R^-$ mediation

According to our observation, although these contributions arising out of mixed effects by the exchanges of light LH and heavy RH neutrinos and also by the exchange of sterile neutrinos are not so dominant compared to those due to $W_L^- - W_L^-$ mediation with sterile neutrino exchanges, as discussed in Sec. 3.1, the amplitudes are stronger than the standard one. The two types of mixed helicity Feynman diagrams [43–45]; (i). λ - mechansim:

coming from one left-handed and one right-handed current (W_L - W_R mediation) shown in Fig. 5.(a), **(ii)**. η – mechanism: arising because of additional possibility of W_L - W_R mixing even though two hadronic currents are left-handed, as shown in Fig. 5.(b), leading to a suppression factor $\tan \zeta_{LR}$. The corresponding Feynman amplitudes for these mixed helicity diagrams are given below

$$\mathcal{A}_\lambda^{LR} \propto \frac{1}{M_{W_L}^2 M_{W_R}^2} (U_\nu)_{ei} \left(\frac{M_D}{M_N} \right)_{ei} \frac{1}{|p|}, \quad (3.14)$$

$$\mathcal{A}_\eta^{LR} \propto \frac{\tan \zeta_{LR}}{M_{W_L}^4} (U_\nu)_{ei} \left(\frac{M_D}{M_N} \right)_{ei} \frac{1}{|p|} \quad (3.15)$$

3.4 Doubly Charged Higgs contribution

Although we have ignored contributions due to exchanges of LH (RH) doubly charged Higgs bosons Δ_L^{--} (Δ_R^{--}) in this work, we present the corresponding amplitudes for the sake of completeness,

$$(i) \quad \mathcal{A}_{\Delta_L}^{LL} \propto \frac{1}{M_{W_L}^4} \frac{1}{M_{\Delta_L}^2} f_L v_L \quad ,$$

$$(ii) \quad \mathcal{A}_{\Delta_R}^{RR} \propto \frac{1}{M_{W_R}^4} \frac{1}{M_{\Delta_R}^2} f_R v_R \quad .$$

As stated in Sec. 2, the masses of Δ_L^{--} and Δ_L^{++} are of the order of the large parity restoration scale which damps out the induced VEV v_L and the corresponding amplitude. The amplitude due to Δ_R^{--} exchange is damped out compared to the standard amplitude as it is $\propto \frac{1}{M_{W_R}^5}$.

3.5 Nuclear matrix elements and normalized effective mass parameters

By now it is well known that different particle exchange contributions for $0\nu 2\beta$ decay discussed above are also modified by the corresponding nuclear matrix elements which depend upon the chirality of the hadronic currents involved [43–45]. Including all relevant contributions except those due to doubly charged Higgs exchanges, and using eqn. (3.6) - eqn. (3.15), we express the inverse half-life in terms of effective mass parameters with proper normalization factors taking into account the nuclear matrix elements [43–45] leading to the half-life prediction

$$\begin{aligned} [T_{1/2}^{0\nu}]^{-1} &= G_{01}^{0\nu} \{ |\mathcal{M}_\nu^{0\nu}|^2 |\eta_\nu|^2 + |\mathcal{M}_N^{0\nu}|^2 |\eta_{N_R}^L|^2 + |\mathcal{M}_N^{0\nu}|^2 |\eta_{N_R}^R|^2 \\ &\quad + |\mathcal{M}_\lambda^{0\nu}|^2 |\eta_\lambda|^2 + |\mathcal{M}_\eta^{0\nu}|^2 |\eta_\eta|^2 \} + \text{interference terms.} \end{aligned} \quad (3.16)$$

where the dimensionless particle physics parameters are

$$\begin{aligned}
|\eta_\nu| &= \left| \frac{\sum_i \mathcal{V}_{ei}^{\nu\nu^2} m_i}{m_e} \right| \\
|\eta_N^R| &= m_p \left(\frac{M_{WL}}{M_{WR}} \right)^4 \left| \frac{\mathcal{V}_{ei}^{NN^2}}{M_{N_i}} \right| \\
|\eta_N^L| &= m_p \left| \frac{V_{ei}^{N\nu}}{M_{N_i}} + \frac{V_{ei}^{S\nu}}{M_{S_i}} \right| \\
|\eta_\lambda| &= \left(\frac{M_{WL}}{M_{WR}} \right)^2 \left| U_{ei} \left(\frac{M_D}{M_N} \right)_{ei} \right| \\
|\eta_\eta| &= \tan \zeta_{LR} \left| U_{ei} \left(\frac{M_D}{M_N} \right)_{ei} \right|
\end{aligned} \tag{3.17}$$

In eqn. (3.17), m_e (m_i)= mass of electron (light neutrino), and m_p = proton mass. In eqn. (3.16), $G_{01}^{0\nu}$ is the the phase space factor and besides different particle parameters, it contains the nuclear matrix elements due different chiralities of the hadronic weak currents such as $(\mathcal{M}_\nu^{0\nu})$ involving left-left chirality in the standard contribution, and due to heavy neutrino exchanges $(\mathcal{M}_\nu^{0\nu})$ involving right-right chirality arising out of heavy neutrino exchange, $(\mathcal{M}_\lambda^{0\nu})$ for the λ - diagram, and $(\mathcal{M}_\eta^{0\nu})$ for the η - diagram . Explicit numerical values of these nuclear matrix elements discussed in ref. [43–45] are given in Table. 4.

Isotope	$G_{01}^{0\nu}$ [10^{-14} yrs $^{-1}$] Refs. [43, 44]	$\mathcal{M}_\nu^{0\nu}$	$\mathcal{M}_N^{0\nu}$	$\mathcal{M}_\lambda^{0\nu}$	$\mathcal{M}_\eta^{0\nu}$
^{76}Ge	0.686	2.58–6.64	233–412	1.75–3.76	235–637
^{82}Se	2.95	2.42–5.92	226–408	2.54–3.69	209–234
^{130}Te	4.13	2.43–5.04	234–384	2.85–3.67	414–540
^{136}Xe	4.24	1.57–3.85	160–172	1.96–2.49	370–419

Table 4: Phase space factors and nuclear matrix elements with their allowed ranges as derived in Refs. [43–45].

In order to arrive at a common normalization factor for all types of contributions, at first we use the expression for inverse half-life for $0\nu 2\beta$ decay process due to only light active Majorana neutrinos, $[T_{1/2}^{0\nu}]^{-1} = G_{01}^{0\nu} |\mathcal{M}_\nu^{0\nu}|^2 |\eta_\nu|^2$. Using the numerical values given in Tab 4, we rewrite the inverse half-life in terms of effective mass parameter

$$[T_{1/2}^{0\nu}]^{-1} = G_{01}^{0\nu} \left| \frac{\mathcal{M}_\nu^{0\nu}}{m_e} \right|^2 |\mathbf{m}_\nu^{\text{ee}}|^2 = 1.57 \times 10^{-25} \text{ yrs}^{-1} \text{ eV}^{-2} |\mathbf{m}_\nu^{\text{ee}}|^2 = \mathcal{K}_{0\nu} |\mathbf{m}_\nu^{\text{ee}}|^2$$

where $\mathbf{m}_\nu^{\text{ee}} = \sum_i (\mathcal{V}_{ei}^{\nu\nu})^2 m_{\nu_i}$. Then the analytic expression for all relevant contributions to effective mass parameters taking into account the respective nuclear matrix elements turns

out to be

$$\left[T_{1/2}^{0\nu}\right]^{-1} = \mathcal{K}_{0\nu} \left[|\mathbf{m}_\nu^{\text{ee}}|^2 + |\mathbf{m}_N^{\text{ee,R}}|^2 + |\mathbf{m}_S^{\text{ee,L}}|^2 + |\mathbf{m}_\lambda^{\text{ee}}|^2 + |\mathbf{m}_\eta^{\text{ee}}|^2 \right] + \dots \quad (3.18)$$

where the ellipses denote interference terms and all other subdominant contributions. In eqn. (3.18), the new effective mass parameters are

$$\mathbf{m}_N^{\text{ee,R}} = \sum_i \left(\frac{M_{W_L}}{M_{W_R}} \right)^4 (\mathcal{V}_{ei}^{NN})^2 \frac{|p|^2}{m_{N_i}} \quad (3.19)$$

$$\mathbf{m}_S^{\text{ee,L}} = \sum_i (\mathcal{V}_{ei}^{\nu S})^2 \frac{|p|^2}{m_{S_i}} \quad (3.20)$$

$$\mathbf{m}_\lambda^{\text{ee}} = 10^{-2} \left(\frac{M_{W_L}}{M_{W_R}} \right)^2 \left| U_{ei} \left(\frac{M_D}{M_N} \dots \right)_{ei} \right| |\mathbf{p}| \quad (3.21)$$

$$\mathbf{m}_\eta^{\text{ee}} = \tan \zeta_{LR} \left| U_{ei} \left(\frac{M_D}{M_N} \dots \right)_{ei} \right| |\mathbf{p}| \quad (3.22)$$

where $|p|^2 = m_e m_p \mathcal{M}_N^{0\nu} / \mathcal{M}_\nu^{0\nu} \simeq (200 \text{ MeV})^2$. It is to be noted that the suppression factor 10^{-2} arises in the λ -diagram as pointed out in refs. [16, 43–45].

4. Numerical estimation of effective mass parameters

Using analytic expression for relevant effective mass parameters given in eqn. (3.16)- eqn. (3.20) and our model parameters discussed in Sec.2, we now estimate the relevant individual contributions numerically.

4.1 Nearly standard contribution

In our model the new mixing matrix $\mathcal{N}_{ei} \equiv \mathcal{V}_{ei}^{\nu\nu} = (1 - \eta) U_\nu$ contains additional non-unitarity effect due to non-vanishing η where

$$\begin{aligned} \mathcal{N}_{e1} &= (1 - \eta_{e1}) U_{11} - \eta_{e2} U_{21} - \eta_{e3} U_{31} \\ \mathcal{N}_{e2} &= (1 - \eta_{e1}) U_{12} - \eta_{e2} U_{22} - \eta_{e3} U_{32} \\ \mathcal{N}_{e3} &= (1 - \eta_{e1}) U_{13} - \eta_{e2} U_{23} - \eta_{e3} U_{33} \end{aligned} \quad (4.1)$$

We estimate numerical values of \mathcal{N}_{ei} using all allowed values of η discussed in Sec.2 and also by using $U \equiv U_{\text{PMNS}}$. Then the effective mass parameter for the $W_L - W_L$ mediation with light neutrino exchanges is found to be almost similar to the standard prediction

$$|m_\nu^{\text{ee}}| \simeq \begin{cases} 0.004 \text{ eV} & \text{NH,} \\ 0.048 \text{ eV} & \text{IH,} \\ 0.23 \text{ eV} & \text{QD.} \end{cases} \quad (4.2)$$

This nearly standard contribution on effective mass parameter is presented by the dashed-green colored lines of Fig. 6 and Fig. 7 for NH neutrino masses, but it is presented by the

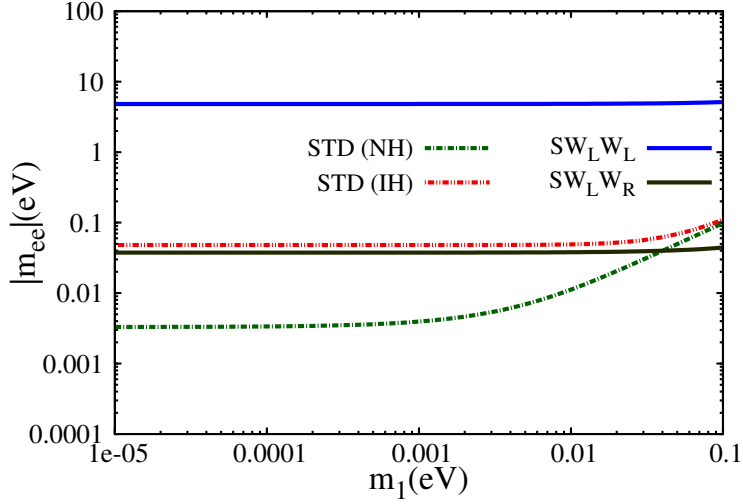


Figure 6: Variation of effective mass parameters with lightest neutrino mass. The standard contributions are shown by dashed-green (pink) colored lines for NH (IH) case. The non-standard contribution with $W_L^- - W_L^-$ mediation and sterile neutrino exchanges is shown by the upper blue solid line whereas the one with $W_L^- - W_R^-$ mediation and sterile neutrino exchanges is shown by the lower black solid line.

dashed-pink colored lines of the same figures for IH neutrino masses. In our numerical estimations presented in Fig.6 we have used M_D values including RG corrections as given in eq.(2.14) but with $M = (50, 200, 1712)$ GeV, $M_N = (1250, 3000, 5000)$ GeV, and $m_{\tilde{g}} = (2, 13, 532)$ GeV. Similarly, in Fig.7 we have utilized M_D values including RG corrections from eq.(2.14) but with $M = (100, 100, 2151.6)$ GeV, $M_N = (5000, 5000, 5000)$ GeV, and $m_{\tilde{g}} = (2, 2, 800)$ GeV.

4.2 Dominant non-standard contributions

Before estimating the non-standard effective mass parameters, we present the mixing matrices numerically. As discussed in eq. (2.13) of Sec. 2, the mixing matrices $X = M_D M^{-1}$, $Y = M M_N^{-1}$, $Z = M_D M_N^{-1}$, and $y = \mu_S M^{-1}$ all contribute to non-standard predictions of $0\nu\beta\beta$ amplitude in the extended seesaw scheme.

Using eqn.(2.13) and the diagonal structures of the RH Majorana neutrino mass matrix $M_N = \text{diag}(M_{N_1}, M_{N_2}, M_{N_3})$ as well as $N - S$ mixing matrix $M = \text{diag}(M_1, M_2, M_3)$, and the Dirac neutrino mass matrix M_D with RG corrections given in eqn. (2.14), we derive the relevant elements of the mixing matrices \mathcal{N} , $\mathcal{V}^{\nu N}$, $\mathcal{V}^{\nu S}$, $\mathcal{V}^{S\nu}$, \mathcal{V}^{SS} , \mathcal{V}^{SN} , $\mathcal{V}^{N\nu}$, \mathcal{V}^{NS} and \mathcal{V}^{NN} for which one example is

$$\begin{aligned}
\mathcal{N}_{ei} &= \{0.8135, 0.5597, 0.1278\}, & \mathcal{V}_{ei}^{\nu S} &= \{4.5398 \times 10^{-4}, 4.93 \times 10^{-4}, 2.148 \times 10^{-4}\}, \\
\mathcal{V}_{ei}^{\nu N} &= \{1.8 \times 10^{-5}, 3.3 \times 10^{-5}, 6.7 \times 10^{-5}\}, & \mathcal{V}_{ei}^{S\nu} &= \{3.6 \times 10^{-3}, 3.3 \times 10^{-3}, 6.0 \times 10^{-3}\}, \\
\mathcal{V}_{ei}^{SS} &= \{0.999, 0.0002, 5.0 \times 10^{-6}\}, & \mathcal{V}_{ei}^{SN} &= \{0.04, 0.0, 0.0\}, & \mathcal{V}_{ei}^{NN} &= \{1.0, 0.0, 0.0\}, \\
\mathcal{V}_{ei}^{N\nu} &= \{9.33 \times 10^{-10}, 2.97 \times 10^{-9}, 1.0 \times 10^{-8}\}, & \mathcal{V}_{ei}^{NS} &= \{0.04, 0.0, 0.0\}. & & (4.3)
\end{aligned}$$

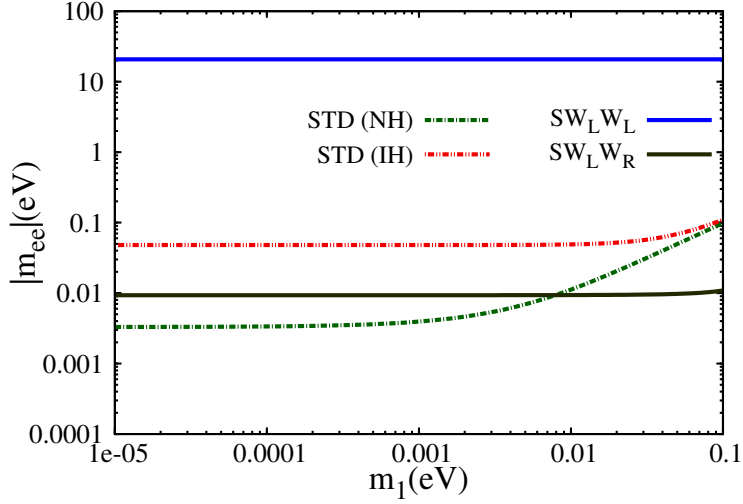


Figure 7: Variation of effective mass parameters with lightest neutrino mass. The standard contributions are shown by dashed-green (pink) colored lines for NH (IH) case. The non-standard contribution with $W_L^- - W_L^-$ mediation and sterile neutrino exchanges is shown by the upper blue solid line whereas the one with $W_L^- - W_R^-$ mediation and sterile neutrino exchanges is shown by the lower black solid line.

For evaluating these mixing matrix elements we have taken the input values, M , M_N ,

C1:	C2:
$M = \text{diag}(50.0, 200.0, 1711) \text{ GeV}$	$M = \text{diag}(100.0, 100.0, 2151.6) \text{ GeV}$
$M_N = \text{diag}(1250.0, 3000.0, 5000.0) \text{ GeV}$	$M_N = \text{diag}(5000.0, 5000.0, 5000.0) \text{ GeV}$
$\hat{m}_S = \text{diag}(2.0, 13.0, 532) \text{ GeV}$	$\hat{m}_S = \text{diag}(2.0, 2.0, 800) \text{ GeV}.$

Table 5: Input values of M , M_N , and \hat{m}_S used for estimating effective mass parameters given in Table 6.

and \hat{m}_S presented under column **C1** of Table. 5. These lead to the numerical results for effective mass parameter contributing to $0\nu\beta\beta$ decay rate presented under column **C1** of TABLE. 6. Similarly when we use the M , M_N , and \hat{m}_S values from column **C2** of Table. 5 we obtain effective mass parameters given in column **C2** of TABLE. 6.

Effective mass parameter	C1 (eV)	C2 (eV)
\mathbf{m}_ν^{ee}	0.004	0.004
$\mathbf{m}_N^{ee,R}$	0.0085	0.0085
$\mathbf{m}_S^{ee,L}$	20.75	188.48
$\mathbf{m}_{\lambda,\eta}^{ee}$	$\simeq 0.0093$	$\simeq 0.0274$

Table 6: Estimations of effective mass parameter with the allowed model parameters. The results are for the Dirac neutrino mass matrix including RG corrections. The input values of mass matrices allowed by the current data for different columns are presented in Table 5.

The most dominant and new contribution to the effective mass parameters is found

to emerge from the amplitude A_S^{LL} of eqn. (3.6) due to $W_L^- - W_L^-$ mediation and sterile neutrino exchanges. This has been shown in Fig. 8 for various combinations of sterile neutrino mass eigenvalues and for M_D values including RG corrections given in eq. (2.14). In Fig. 8 our estimated values range from 0.2 eV-1.0 eV. Looking to the results given in Table. 6 and Fig. 6, Fig. 7, and Fig. 8, it is clear that the actual enhanced rate of $0\nu\beta\beta$ decay in this model depends primarily upon the sterile neutrino mass eigenvalues m_{S_1} and m_{S_2} . If the decay rate corresponds to $|M_{\text{eff}}| \simeq 0.21 - 0.53$ eV as claimed by the Heidelberg-Moscow experiment using ${}^{76}\text{Ge}$ [11], our new finding is that the light neutrino masses could be still of NH or IH pattern, instead of necessarily being of QD pattern, but with $m_{S_1} \sim 10$ GeV and $m_{S_2} \sim 30$ GeV. Of course the Dirac neutrino mass matrix having its high scale quark-lepton symmetric origin also contributes to the magnification of the effective mass parameter. The next dominant contributions coming from the Feynman amplitude A_S^{LR} of eqn. (3.15) due to $W_L^- - W_R^-$ mediation and sterile neutrino exchanges with $m_{\lambda,\eta}^{\text{ee,LR}} = 0.04$ eV (0.01 eV) have been shown in Fig. 6 (Fig. 7).

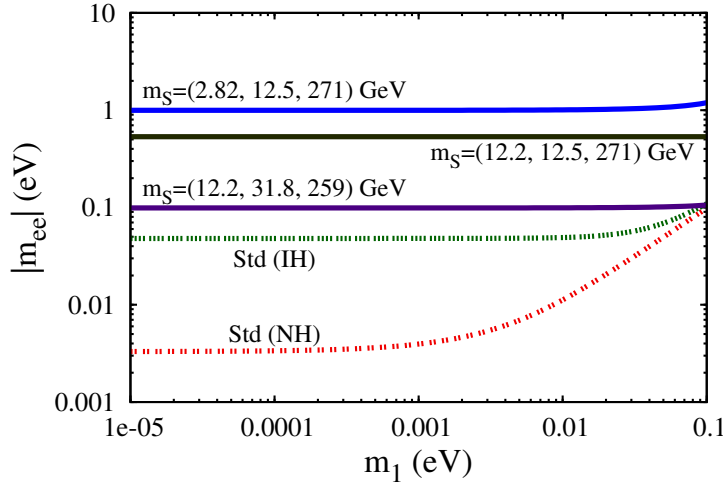


Figure 8: Predictions of non-standard contributions to effective mass parameter with $W_L^- - W_L^-$ mediation and sterile neutrino exchange for $M = (120, 250, 1664.9)$ GeV (top solid line), $M = (250, 250, 1663.3)$ GeV (middle solid line), and $M = (250, 400, 1626.1)$ GeV (bottom solid line) keeping $M_N = (5, 5, 10)$ TeV fixed and for M_D as in eq. (2.14).

5. Estimations on lepton flavor violating decays and J_{CP}

Besides the neutrinoless double beta decay process, the sterile and heavy neutrinos in this model can predominantly mediate different lepton flavor violating decays, $\mu \rightarrow e + \gamma$, $\tau \rightarrow e + \gamma$, and $\tau \rightarrow \mu + \gamma$. Since $\ell_\alpha \rightarrow \ell_\beta + \gamma$ ($\alpha \neq \beta$) is lepton flavor changing process, it is strictly forbidden in the Standard Model when $m_\nu = 0$ and lepton number is conserved. In our model the underlying lepton-flavor violating interactions and non-unitarity effects contribute to LFV decays by the mediation of heavy RH Majorana and sterile Majorana fermions.

$M(\text{GeV})$	$M_N(\text{TeV})$	Heavy Mass Eigen Values(GeV)
(9.7, 115.2, 2776.5)	(5, 5, 5)	(0.018, 2.65, 1238, 5000, 5002, 6238)
(100, 100,2151.57)	(5, 5, 5)	(1.99, 2.00, 800.5, 5001, 5002, 5800)
(100, 200, 1702.67)	(5, 5, 5)	(1.99, 8.00, 527.5, 5001, 5007, 5527)
(50, 200,1711)	(1.5, 2, 5)	(1.67, 19.8, 532.2, 1501, 2019, 5532)
(1604.442,1604.442,1604.442)	(5,5,10)	(252.4,461.5,470.6,5471.56,5471.35,10252.4)

Table 7: The Heavy mass eigen values for the matrices of M and M_N which have been used to evaluate branching ratios.

5.1 Branching ratio

Keeping in mind the charged-current interaction in the neutrino mass basis for extended seesaw scheme given in eq. (3.1) - eq. (3.3), the dominant contributions are mainly through the exchange of the sterile and heavy RH neutrinos with branching ratio [28, 46]

$$\text{Br}(\ell_\alpha \rightarrow \ell_\beta + \gamma) = \frac{\alpha_w^3 s_w^2 m_{\ell_\alpha}^5}{256 \pi^2 M_W^4 \Gamma_\alpha} |\mathcal{G}_{\alpha\beta}^N + \mathcal{G}_{\alpha\beta}^S|^2, \quad (5.1)$$

$$\text{where } \mathcal{G}_{\alpha\beta}^N = \sum_k (\nu^{\nu N})_{\alpha k} (\nu^{\nu N})_{\beta k}^* \mathcal{I}\left(\frac{m_{N_k}^2}{M_{WL}^2}\right),$$

$$\mathcal{G}_{\alpha\beta}^S = \sum_j (\nu^{\nu S})_{\alpha j} (\nu^{\nu S})_{\beta j}^* \mathcal{I}\left(\frac{m_{S_j}^2}{M_{WL}^2}\right),$$

$$\text{and } \mathcal{I}(x) = -\frac{2x^3 + 5x^2 - x}{4(1-x)^3} - \frac{3x^3 \ln x}{2(1-x)^4}.$$

It is clear from the above equation and within the model parameter range, $M_N \gg M \gg M_D$, that the first term in eq. (5.1) is negligible while second term involving the the heavy sterile neutrinos gives dominant contribution which is proportional to $\sum_j (\nu^{\nu S})_{\alpha j} (\nu^{\nu S})_{\beta j}^* \simeq 2\eta_{\alpha\beta}$.

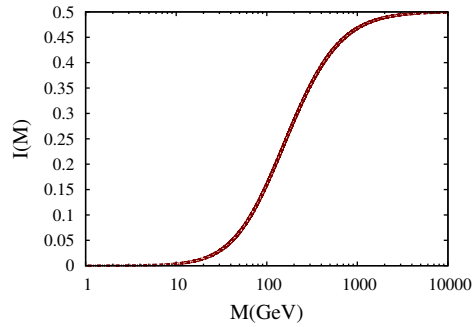


Figure 9: Loop factor vs masses of heavy RH or sterile neutrino.

Taking into account the contribution of the non-unitarity matrix, it is clear that out of diagonal elements of M_N and M , mostly the latter contributes to the branching ratios.

Also the contribution of loop factor for various range of masses allowed in this extended seesaw mechanism is shown in Fig. 9.

$M(\text{GeV})$	$M_N(\text{TeV})$	$\text{Br}(\mu \rightarrow e\gamma)$	$\text{Br}(\tau \rightarrow e\gamma)$	$\text{Br}(\tau \rightarrow \mu\gamma)$
(50, 200, 1711.8)	(1.5, 2, 5)	3.05×10^{-16}	3.11×10^{-14}	4.36×10^{-12}
(100, 100, 2151.57)	(5, 5, 5)	1.28×10^{-16}	1.39×10^{-14}	1.95×10^{-12}
(100, 200, 1702.67)	(5, 5, 5)	2.85×10^{-16}	3.1×10^{-14}	4.3×10^{-12}
(1604.442, 1604.442, 1604.442)	(5, 5, 10)	2.18×10^{-16}	2.32×10^{-14}	3.25×10^{-12}

Table 8: The three branching ratios in extended inverse seesaw for different values of M and M_N while M_D is same as in eq. (2.14).

Using the numerically computed mixing matrix, and using allowed mass scales presented in Table 7, our model estimations on branching ratios are given in Table 8. Recent experimental data gives the best limit on these branching ratios for LFV decays coming from the MEG collaboration [47]. Out of these $\text{Br}(\mu \rightarrow e + \gamma) \leq 1.2 \times 10^{-11}$ [47] is almost three orders of magnitude stronger than the limit $\text{Br}(\tau \rightarrow e + \gamma) \leq 3.3 \times 10^{-8}$ or $\text{Br}(\tau \rightarrow \mu + \gamma) \leq 4.4 \times 10^{-8}$ at 90% C.L. However, projected reach of future sensitivities of ongoing searches are $\text{Br}(\tau \rightarrow e + \gamma) \leq 10^{-9}$, $\text{Br}(\tau \rightarrow \mu + \gamma) \leq 10^{-9}$, and $\text{Br}(\mu \rightarrow e + \gamma) \leq 10^{-18}$ [47] which might play crucial role in verifying or falsifying the discussed scenario.

5.2 CP-violation due to non-unitarity

There are attempts taken in long baseline experiments [13] with accelerator neutrinos ν_μ and anti-neutrinos $\bar{\nu}_\mu$ to search for CP violating effects in neutrino oscillations. In the usual notation, the standard contribution to these effects is determined by the rephasing invariant J_{CP} associated with the Dirac phase δ_{CP} and matrix elements of the PMNS matrix

$$J_{\text{CP}} \equiv \text{Im} (U_{\alpha i} U_{\beta j} U_{\alpha j}^* U_{\beta i}^*) = \cos \theta_{12} \cos^2 \theta_{13} \cos \theta_{23} \sin \theta_{12} \sin \theta_{13} \sin \theta_{23} \sin \delta_{\text{CP}}.$$

In this extended seesaw mechanism, the leptonic CP-violation can be written as

$$\mathcal{J}_{\alpha\beta}^{ij} = \text{Im} (\mathcal{N}_{\alpha i} \mathcal{N}_{\beta j} \mathcal{N}_{\alpha j}^* \mathcal{N}_{\beta i}^*) \simeq J_{\text{CP}} + \Delta J_{\alpha\beta}^{ij} \quad (5.2)$$

where [36, 37, 39, 40]

$$\Delta J_{\alpha\beta}^{ij} = - \sum_{\rho=e,\mu,\tau} \text{Im} \left[\eta_{\alpha\rho} U_{\rho i} U_{\beta j} U_{\alpha j}^* U_{\beta i}^* + \eta_{\beta\rho} U_{\alpha i} U_{\rho j} U_{\alpha j}^* U_{\beta i}^* \right. \\ \left. + \eta_{\alpha\rho}^* U_{\alpha i} U_{\beta j} U_{\rho j}^* U_{\beta i}^* + \eta_{\beta\rho}^* U_{\alpha i} U_{\beta j} U_{\alpha j}^* U_{\rho j}^* \right]. \quad (5.3)$$

The extra contribution arises because of the non-unitarity mixing matrix which depends on both M_D and M . Thus the new contribution to CP-violation is larger for larger M_D which is generated with quark-lepton symmetry and for smaller M while safeguarding the constraint $M_N \gg M > M_D, \mu_S$. It is noteworthy that in our model even if the leptonic

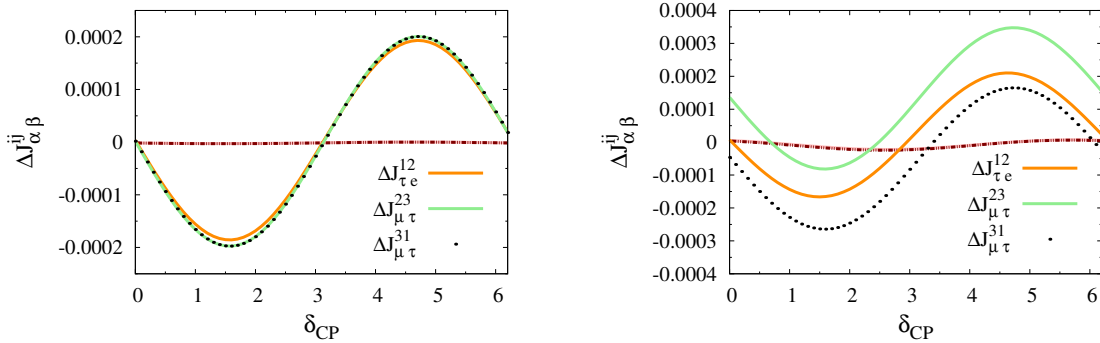


Figure 10: CP-violation for the full allowed range of leptonic Dirac phase δ_{CP} . The left-panel corresponds to degenerate values of M with $M_1 = M_2 = M_3 \simeq 1604.442$ GeV, and the right panel is due to non-degenerate M with $M_1 = 9.7$ GeV, $M_2 = 115.2$ GeV, and $M_3 = 2776.5$ GeV.

M	$\Delta \mathcal{J}_{e\mu}^{12}$	$\Delta \mathcal{J}_{e\mu}^{23}$	$\Delta \mathcal{J}_{\mu\tau}^{23}$	$\Delta \mathcal{J}_{\mu\tau}^{31}$	$\Delta \mathcal{J}_{\tau e}^{12}$
(a)	-2.0×10^{-6}	-2.3×10^{-6}	-1.2×10^{-4}	-1.2×10^{-4}	-1.1×10^{-4}
(b)	-2.7×10^{-6}	-3.2×10^{-6}	-1.2×10^{-4}	-1.2×10^{-4}	-1.1×10^{-4}
(c)	-2.1×10^{-5}	-2.4×10^{-5}	1.1×10^{-7}	-1.8×10^{-4}	-7.9×10^{-5}

Table 9: The CP-violating effects for (a) degenerate masses $M = (1604.442, 1604.442, 1604.442)$ GeV, (b) partially degenerate masses $M = (100, 100, 2151.57)$ GeV and (c) non degenerate masses $M = (9.7, 115.2, 2776.5)$ GeV, while M_D is same as in eq. (2.14).

Dirac phase $\delta_{CP} \simeq 0, \pi, 2\pi$, and/or $\sin \theta_{13} \rightarrow 0$, there is substantial contribution to CP-violation which might arise out of the imaginary parts of the non-unitarity matrix elements $\eta_{\alpha\beta}$.

Our estimations using RG corrected Dirac neutrino mass matrix and both degenerate and non-degenerate matrix M are shown in the left-panel and right-panel of Fig. 10. If the leptonic Dirac phase $\delta_{CP} \neq 0, \pi, 2\pi$, significant CP-violation up to $|\Delta J|_{\max} \simeq 1.5 \times 10^{-4}$ is found to occur for degenerate M , but when M is non-degenerate we obtain $|\Delta J|_{\max} \simeq (2 - 4) \times 10^{-4}$. Also even if $\delta_{CP} \simeq 0, \pi, 2\pi$, non-vanishing CP-violation to the extent of $|\Delta J| \simeq (1 - 2) \times 10^{-4}$ is noted to emerge for non-degenerate M . These results may be compared with CP-violation in the quark sector where $\mathcal{J}_{CKM} \simeq 3.05_{-0.20}^{+0.19} \times 10^{-5}$ [33] which is nearly one order lower than the leptonic case. The horizontal lines in Fig. 10 represent absence of non-unitarity effects on CP-violation.

6. Implementation in SO(10)

Our main goal in this section is to examine whether the TeV scale LR gauge model that has been shown to give rise to dominant contribution to $0\nu\beta\beta$ decay and lepton flavor violation in Sec.2 - Sec.5 can emerge from a non-SUSY SO(10) grand unified theory. Although the search for low mass W_R^\pm bosons in non-SUSY GUTs has been attempted initially without

[48] precision CERN-LEP data on $\alpha_S(M_Z)$ and $\sin^2 \theta_W(M_Z)$ [33], there are more recent results on physically appealing intermediate scales [18, 49]. But the analyses in non-SUSY cases where the $B - L$ breaking scale synonymous to W_R gauge boson mass much lower than 10^{10} GeV are ruled out because of the associated large contributions to light neutrino masses via type-I seesaw mechanism. In view of the rich phenomenological consequences of the extended seesaw mechanism that evades the discordance between dominant $0\nu\beta\beta$ decay and small neutrino mass predictions as discussed in Sec.2 - Sec.5, we explore the possibility of such low scale LR gauge theory in the minimally extended $SO(10)$ grand unification model.

6.1 Symmetry breaking chain

We consider the symmetry breaking chain discussed in Ref. [18]. Although this model, as such, is ruled out because of the TeV scale canonical seesaw that operates to give large neutrino masses in contravention of the oscillation data, here we modify this model by including the additional doublets $(\chi_L, \chi_R) \subset 16_H$ of $SO(10)$ and extending the minimal fermion content in $\{16\}_F$ with the addition of one $SO(10)$ singlet neutral fermion per generation in order to implement the extended seesaw mechanism

$$\begin{aligned}
SO(10) &\xrightarrow[\{54\}]{M_U} SU(2)_L \times SU(2)_R \times SU(4)_C \times D && [\mathcal{G}_{224D}, (g_{2L} = g_{2R})] \\
&\xrightarrow[\{210\}]{M_P} SU(2)_L \times SU(2)_R \times SU(4)_C && [\mathcal{G}_{224}, (g_{2L} \neq g_{2R})] \\
&\xrightarrow[\{210\}]{M_C} SU(2)_L \times SU(2)_R \times U(1)_{B-L} \times SU(3)_C && [\mathcal{G}_{2213}] \\
&\xrightarrow[\{210\}]{M_R^+} SU(2)_L \times U(1)_R \times U(1)_{B-L} \times SU(3)_C && [\mathcal{G}_{2113}] \\
&\xrightarrow[\{126+16\}]{M_R^0} SU(2)_L \times U(1)_Y \times SU(3)_C && [\mathcal{G}_{SM}] \\
&\xrightarrow[\{10\}]{M_Z} U(1)_{em} \times SU(3)_C. && (6.1)
\end{aligned}$$

It was found that the G_{224} -singlets in $\{54\}_H$ and $\{210\}_H$ of $SO(10)$ are D-parity even and odd, respectively. Also it was noted that the neutral components of the G_{224} multiplet $\{1, 1, 15\}$ contained in $\{210\}_H$ and $\{45\}_H$ of $SO(10)$ have D-parity even and odd, respectively. In the first step, VEV is assigned along the $\langle(1, 1, 1)\rangle \subset \{54\}_H$ which has even D-Parity to guarantee the LR symmetric Pati-Salam group to survive while at the second step D-parity is broken by assigning $\langle(1, 1, 1)\rangle \subset \{210\}_H$ to obtain asymmetric G_{224} with $g_{2L} \neq g_{2R}$. The spontaneous breaking $G_{224} \rightarrow G_{2213}$ is achieved by the VEV $\langle(1, 1, 15)_H^0\rangle \subset \{210\}_H$. The symmetry breaking $G_{2213} \rightarrow G_{2113}$ is implemented by assigning $O(M_R^+)$ VEV to the neutral component of the sub-multiplet $\langle(1, 3, 15)_H^0\rangle \subset \{210\}_H$, and the breaking $U(1)_R \times U(1)_{B-L} \rightarrow U(1)_Y$ is achieved by $\langle\Delta_R^0\rangle \subset \{126\}_H$ while the VEV $\langle\chi_R^0\rangle \subset \{16\}_H$ provides the N - S mixing. As usual, the breaking of SM to low energy symmetry $U(1)_{em} \times SU(3)_C$ is carried out by the SM doublet contained in the bidoublet $\Phi \subset \{10\}_H$.

6.2 Gauge coupling unification

We have evaluated the one-loop and two-loop coefficients of β -functions of renormalization group equations for the gauge couplings [50]

$$\mu \frac{\partial g_i}{\partial \mu} = \frac{a_i}{16\pi^2} g_i^3 + \frac{1}{16\pi^2} \sum_j b_{ij} g_i^3 g_j^2, \quad (6.2)$$

and they are given in Table. 12 of appendix.

The Higgs spectrum used in different ranges of mass scales under respective gauge symmetries (G) are

$$\begin{aligned}
\text{(i)} \quad \mu = \mathbf{M}_Z - \mathbf{M}_R^0 : G = \text{SM} = G_{213}, \quad & \Phi(2, 1/2, 1); \\
\text{(ii)} \quad \mu = \mathbf{M}_R^0 - \mathbf{M}_R^+ : G = G_{2113}, \quad & \Phi_1(2, 1/2, 0, 1) \oplus \Phi_2(2, -1/2, 0, 1) \oplus \\
& \chi_R(1, 1/2, -1, 1) \oplus \Delta_R(1, 1, -2, 1); \\
\text{(iii)} \quad \mu = \mathbf{M}_R^+ - \mathbf{M}_C : G = G_{2213}, \quad & \Phi_1(2, 2, 0, 1) \oplus \Phi_2(2, 2, 0, 1) \oplus \\
& \chi_R(1, 2, -1, 1) \oplus \Delta_R(1, 3, -2, 1) \oplus \Sigma_R(1, 3, 0, 1); \\
\text{(iv)} \quad \mu = \mathbf{M}_C - \mathbf{M}_P : G = G_{224}, \quad & \Phi_1(2, 2, 1) \oplus \Phi_2(2, 2, 1) \oplus \\
& \chi_R(1, 2, \bar{4}) \oplus \Delta_R(1, 3, \bar{10}) \oplus \Sigma_R(1, 3, 15); \\
\text{(v)} \quad \mu = \mathbf{M}_P - \mathbf{M}_U : G = G_{224D}, \quad & \Phi_1(2, 2, 1) \oplus \Phi_2(2, 2, 1) \oplus \\
& \chi_L(2, 1, 4) \oplus \chi_R(1, 2, \bar{4}) \oplus \\
& \Delta_L(3, 1, 10) \oplus \Delta_R(1, 3, \bar{10}) \oplus \\
& \Sigma_L(3, 1, 15) \oplus \Sigma_R(1, 3, 15). \quad (6.3)
\end{aligned}$$

Recently bounds on the masses of the charged and neutral components of the second Higgs doublet in the left-right symmetric model has been estimated to be $O(20)$ TeV [58]. While searching for possible mass scales we have used the second Higgs doublet Φ_2 only for $\mu \geq 10$ TeV.

We have used extended survival hypothesis in implementing spontaneous symmetry breaking of $SO(10)$ and intermediate gauge symmetries leading to the SM gauge theory [51, 52]. In addition to D-Parity breaking models [17, 18], the importance of the Higgs representation 210_H has been emphasized in the construction of a minimal supersymmetric $SO(10)$ GUT model [53]. But the present non-SUSY $SO(10)$ symmetry breaking chain

M_R^0 (TeV)	M_R^+ (TeV)	M_C (TeV)	M_P (GeV)	M_G (GeV)	α_G
5	10	10^3	$10^{14.2}$	$10^{17.64}$	0.03884
5	10	$10^{3.5}$	$10^{14.42}$	$10^{17.61}$	0.03675
5	20	10^3	$10^{14.08}$	$10^{17.54}$	0.03915
5	10	100	$10^{13.72}$	$10^{17.67}$	0.0443
5	20	500	$10^{13.93}$	$10^{17.55}$	0.0406

Table 10: Predictions of allowed mass scales and the GUT couplings in the $SO(10)$ symmetry breaking chain with low-mass W_R^\pm, Z_R bosons.

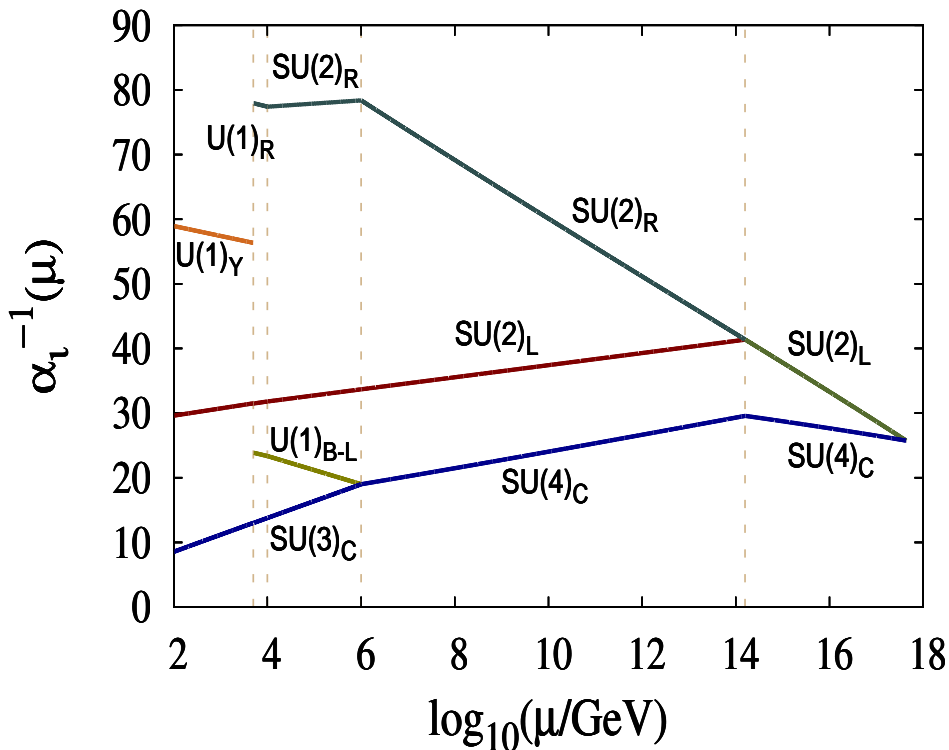


Figure 11: Two loop gauge coupling unification in the $SO(10)$ symmetry breaking chain described in the text. These results are also valid with G_{224D} symmetry near GUT-Planck scale.

shows a departure in that the G_{224D} symmetry essentially required at the highest intermediate scale has unbroken D-Parity which is possible by breaking the GUT symmetry through the Higgs representation $54_H \subset SO(10)$ that acquires GUT-scale VEV in the direction of its D-parity even G_{224D} -singlet. The importance of this G_{224D} symmetry in stabilizing the values of M_P and $\sin^2 \theta_W(M_Z)$ against GUT-Planck scale threshold effects has been discussed in ref. [57] and Sec. 6.4 below.

Using precision CERN-LEP data [33] $\alpha_S(M_Z) = 0.1184$, $\sin^2 \theta_W(M_Z) = 0.2311$ and $\alpha^{-1}(M_Z) = 127.9$, different allowed solutions presented in Table. 10. One set of solutions corresponding to low mass W_R^\pm and Z_R gauge bosons is

$$\begin{aligned}
 M_R^0 &= 3 - 5 \text{ TeV}, \quad M_R^+ = 10 \text{ TeV}, \quad M_C = 10^2 \text{ TeV} - 10^3 \text{ TeV}, \\
 M_P &\simeq 10^{14.17} \text{ GeV} \quad \text{and} \quad M_G \simeq 10^{17.8} \text{ GeV}.
 \end{aligned}
 \tag{6.4}$$

For these mass scales the emerging pattern of gauge coupling unification is shown in Fig. 11 with GUT fine structure constant $\alpha_G = 0.0388$.

6.3 Physical significance of mass scales

The presence of G_{224D} symmetry above the highest intermediate scale plays a crucial role in lowering down the values of M_R^+ while achieving high scale gauge coupling unification.

With the gauge couplings allowed in the region $\mu \simeq 3$ TeV - 10 TeV in the grand unified scenario with $g_{B-L} \simeq 0.725$, $g_{2R} \simeq 0.4$, we have estimated the predicted W_R and Z_R masses to be $M_{W_R} \simeq 4$ TeV, $M_{Z_R} \simeq (2.3 - 3.6)$ TeV for the allowed mass scales $M_R^0 \simeq (3 - 5)$ TeV, and $M_R^{\pm} \simeq 10$ TeV of Table. 10. These low mass W_R and Z_R bosons have interesting RH current effects at low energies including K_L - K_S mass difference and dominant $0\nu\beta\beta$ rates as discussed in Sec. 3- Sec. 5. The predicted low mass W_R^{\pm} and Z_R bosons are also expected to be testified at the LHC and future accelerators for which the current bounds are $M_{W_R} \geq 2.5$ TeV [21, 22] and $M_{Z_R} \geq 1.162$ TeV [24, 25]. The predicted mass scale $M_C \sim (10^5 - 10^6)$ GeV leads to experimentally verifiable branching ratios for rare kaon decay with $\text{Br}(K_L^0 \rightarrow \mu\bar{e}) \simeq (10^{-9} - 10^{-11})$ [27] via leptoquark gauge boson mediation [32]. Because of the presence of \mathcal{G}_{224} symmetry for $\mu \geq M_C$ ($10^5 - 10^6$) GeV, all the components of diquark Higgs scalars in $\Delta_R(3, 1, \bar{10})$ mediating $n - \bar{n}$ and $H - \bar{H}$ oscillations also acquire masses at that scale whereas the dilepton Higgs scalar carrying $B-L = -2$ is at the $\simeq 1$ TeV scale. This gives rise to observable $n - \bar{n}$ oscillation with mixing time $\tau_{n-\bar{n}} \simeq (10^8 - 10^{11})$ secs [26, 54]. However because of the large value of the GUT scale $M_G \simeq 10^{18}$ GeV, which is close to the Planck scale, the predicted proton life time for $p \rightarrow e^+ \pi^0$ is large, i.e. $\tau_p \geq 10^{40}$ yrs which is beyond the accessible range of ongoing search experiments that have set the lower limit $(\tau_p)|_{\text{expt.}} \geq 1.1 \times 10^{34}$ yrs [55].

6.4 Importance of \mathcal{G}_{224D} intermediate symmetry

Near Planck scale unification of this model exposes an interesting possibility that grand unification can be also achieved by the Pati-Salam symmetry \mathcal{G}_{224D} even without the help of the GUT-gauge group $SO(10)$ since, above this scale, gravity effects are expected to take over [56].

The most interesting role of G_{224D} gauge symmetry at the highest intermediate scale has been pointed out in Ref. [57]. Normally super-heavy Higgs scalars contained in larger representations like $\{210\}_H$ and $\{126\}_H$ introduce uncertainties into GUT predictions of $\sin^2 \theta_W(M_Z)$ on which CERN-LEP data and others have precise experimental results. But the presence of G_{224D} at the highest scale achieves the most desired objective that the GUT scale corrections to $\sin^2 \theta_W(M_Z)$ vanish due to such sources as super-heavy particles or higher dimensional operators signifying the effect of gravity.

6.5 Determination of Dirac neutrino mass matrix

It is well known that within Pati-Salam gauge symmetry \mathcal{G}_{224D} , the presence of $SU(4)_C$ unifies quarks and leptons treating the latter as fourth color and this relates the up-quark mass matrix (M_u^0) to the Dirac neutrino mass matrix M_D^0 at the unification scale. Such relations are also valid in $SO(10)$ at the GUT scale since \mathcal{G}_{224D} is its maximal subgroup. Over the recent years it has been shown that in a large class of $SO(10)$ model the fermion mass fits at the GUT scale gives $M_D^0 \sim \mathcal{O}(M_u^0)$ [35-37]. Since the predictions of lepton number and lepton flavor violations carried out in this work are sensitive to the Dirac neutrino mass matrix, it is important to derive M_D at the TeV scale given in eq. (2.14). This question has been answered in non-SUSY $SO(10)$ [37] and SUSY $SO(10)$ [36] while utilizing renormalization group running of fermion masses analogous to ref. [34] and using

their low energy data but in the presence of intermediate symmetries G_{2113} , G_{2213} , and G_{2213D} . In this analysis we will also use additional RGEs for Yukawa coupling and fermion masses in the presence of G_{224} and G_{224D} symmetries operating between $M_C \simeq 10^5$ GeV to $M_{\text{GUT}} \simeq 10^{17.5}$ GeV [59].

The determination of the Dirac neutrino mass matrix $M_D(M_{R^0})$ at the TeV seesaw scale is done in three steps [37]: **(A.)** Extrapolation of masses to the GUT-scale using low-energy data on fermion masses and CKM mixings through corresponding RGEs in the bottom-up approach, **(B.)** Fitting the fermion masses at the GUT scale and determination of $M_D(M_{\text{GUT}})$, **(C.)** Determination of $M_D(M_{R^0})$ by top-down approach.

A. Extrapolation of fermion masses to the GUT scale

At first RGEs for Yukawa coupling matrices and fermion mass matrices are set up from which RGEs for mass eigen values and CKM mixings are derived in the presence of G_{2113} , G_{2213} , G_{224} , and G_{224D} symmetries.

Denoting $\Phi_{1,2}$ as the corresponding bidoublets under G_{2213} their VEVs are taken as

$$\begin{aligned}\langle\Phi_1\rangle &= \begin{pmatrix} v_u & 0 \\ 0 & 0 \end{pmatrix}, \\ \langle\Phi_2\rangle &= \begin{pmatrix} 0 & 0 \\ 0 & v_d \end{pmatrix}.\end{aligned}\tag{6.5}$$

For mass scales $\mu \ll M_G$, ignoring the contribution of the superheavy bidoublet in 126_H , the bidoublet $\Phi_1 \subset 10_{H_1}$ is assumed to give dominant contribution to up quark and Dirac neutrino masses M_u and M_D whereas $\Phi_2 \subset 10_{H_2}$ is used to generate masses for down quarks and charged leptons, M_d and M_ℓ

$$\begin{aligned}M_u &= Y_u v_u, & M_D &= Y_\nu v_u, & M_d &= Y_d v_d, \\ M_e &= Y_e v_d, & M_R &= y_\chi v_\chi,\end{aligned}\tag{6.6}$$

At $\mu = M_Z$ we use the input values of running masses and quark mixings as in ref. [34]

$$\begin{aligned}m_e &= 0.48684727 \pm 0.00000014 \text{ MeV}, & m_\mu &= 102.75138 \pm 0.00033 \text{ MeV}, \\ m_\tau &= 1.74669_{-0.00027}^{+0.00030} \text{ GeV}, & m_d &= 4.69_{-0.66}^{+0.60} \text{ MeV}, \\ m_s &= 93.4_{-13.0}^{+11.8} \text{ MeV}, & m_b &= 3.00 \pm 0.11 \text{ GeV}, \\ m_u &= 2.33_{-0.45}^{+0.42} \text{ MeV}, & m_c &= 677_{-51}^{+56} \text{ MeV}, \\ m_t &= 181 \pm 1.3 \text{ GeV}, \\ \theta_{12}^q &= 13.04^\circ \pm 0.05^\circ, & \theta_{13}^q &= 0.201^\circ \pm 0.201^\circ, \\ \theta_{23}^q &= 2.38^\circ \pm 0.06^\circ,\end{aligned}\tag{6.7}$$

with the CKM Dirac phase $\delta^q = 1.20 \pm 0.08$. This results in the CKM matrix at $\mu = M_Z$

$$V_{\text{CKM}} = \begin{pmatrix} 0.9742 & 0.2256 & 0.0013 - 0.0033i \\ -0.2255 + 0.0001i & 0.9734 & 0.04155 \\ 0.0081 - 0.0032i & -0.0407 - 0.0007i & 0.9991 \end{pmatrix}.\tag{6.8}$$

We use RGEs of the standard model [34] to evolve all charged fermion masses and CKM mixings from $\mu = M_Z$ to $M_R^0 \simeq 10$ TeV. With two Higgs doublets at $\mu > 10$ TeV consistent with the current experimental lower bound on the second Higgs doublet [58], we use the starting value of $\tan\beta = v_u/v_d = 10$ and evolve the masses up to $\mu = M_C$ using RGEs derived in the presence of non-SUSY $SO(10)$ and intermediate symmetries G_{2113} and G_{2213} [37] with two Higgs bidoublets. For $\mu \geq M_C$, we use the fermion mass RGEs in the presence of G_{224} and G_{224D} [59] modified including the corresponding RGEs of v_u and v_d . The fermion mass eigen values m_i and the V_{CKM} at the GUT scale turn out to be

At $\mu = M_{\text{GUT}}$ scale:

$$\begin{aligned} m_e^0 &= 0.2168 \text{ MeV}, m_\mu^0 = 38.846 \text{ MeV}, m_\tau^0 = 0.9620 \text{ GeV}, \\ m_d^0 &= 1.163 \text{ MeV}, m_s^0 = 23.352 \text{ MeV}, m_b^0 = 1.0256 \text{ GeV}, \\ m_u^0 &= 1.301 \text{ MeV}, m_c^0 = 0.1686 \text{ GeV}, m_t^0 = 51.504 \text{ GeV}, \end{aligned} \quad (6.9)$$

$$V_{\text{CKM}}^0(M_{\text{GUT}}) = \begin{pmatrix} 0.9764 & 0.2160 & -0.00169 - 0.00356i \\ -0.2159 - 0.0001i & 0.9759 - 0.00002i & 0.0310 \\ 0.00835 - 0.00348i & -0.02994 - 0.00077i & 0.9995 \end{pmatrix}, \quad (6.10)$$

where, in deriving eqn. (6.9), we have used ‘‘run and diagonalize procedure. Then using eqn. (6.9) and eqn. (6.10), the RG extrapolated value of the up-quark mass matrix at the GUT scale is determined

$$M_u^0(M_{\text{GUT}}) = \begin{pmatrix} 0.00973 & 0.0379 - 0.00693i & 0.0635 - 0.1671i \\ 0.0379 + 0.00693i & 0.2482 & 2.117 + 0.000116i \\ 0.0635 + 0.1672i & 2.117 - 0.000116i & 51.38 \end{pmatrix} \text{ GeV}. \quad (6.11)$$

B. Determination of M_D at GUT scale

In order to fit the fermion masses at the GUT scale, in addition to the two bidoublets originating from two different Higgs representations 10_{H_1} and 10_{H_2} , we utilize the superheavy bidoublet in $\xi(2, 2, 15) \subset 126_H$. We will show that even if ξ has to be at the intermediate scale ($10^{13} - 10^{14}$) GeV to generate the desired value of induced VEV needed for quark-lepton mass splitting, the precision gauge coupling unification is unaffected. This fermion mass requires the predicted Majorana coupling f to be diagonal and the model predicts experimentally testable RH neutrino masses. In the presence of inverse seesaw formula taking into account the small masses and large mixings in the LH neutrino sector in the way of fitting the neutrino oscillation data, this diagonal structure of f causes no problem. However we show that when we treat the intermediate scale for sub-multiplet to be $\xi'(2, 2, 15)$ replacing $\xi(2, 2, 15)$ but originating from a second Higgs representation $126'_H$ which has coupling f' to the fermions and all other scalar components at the GUT scale, the coupling f and hence M_N can have a general texture, not necessarily diagonal, although fermion mass fit needs only f' to be diagonal.

The VEV of $\xi(2, 2, 15)$ is well known for its role in to splitting the quark and lepton masses through the Yukawa interaction $f\mathbf{16.16.126}_H^\dagger$ [60]. It is sometimes apprehended, as happens in the presence of only one 10_H , that this new contribution may also upset the near equality of $M_u^0 \simeq M_D^0$ at the GUT scale. But in the presence of the two different 10_{H_1} and 10_{H_2} producing the up and down type doublets, the effective theory from the $\mu \geq 10$ TeV acts like a nonsupersymmetric two-Higgs doublet model with available large value of $\tan \beta = v_u/v_d$ that causes the most desired splitting between the up and down quark mass matrices but ensures $M_u^0 \sim M_D^0$. After having achieved this splitting a smaller value of of the VEV v_ξ is needed to implement fitting of charged fermion mass matrices without substantially upsetting the near equality of $M_u^0 \simeq M_D^0$ at the GUT scale *.

The formulas for mass matrices at the GUT scale are [36,37]

$$\begin{aligned} M_u &= G_u + F, & M_d &= G_d + F, \\ M_e &= G_d - 3F, & M_D &= G_u - 3F. \end{aligned} \quad (6.12)$$

where $G_k = Y_k \langle 10_H^k \rangle$, $k = u, d$ and $F = f v_\xi$ leading to

$$f = \frac{(M_d - M_e)}{4v_\xi}. \quad (6.13)$$

Using a charged-lepton diagonal mass basis and eq. (6.9) and eq. (6.12) we have

$$\begin{aligned} M_e(M_{GUT}) &= \text{diag}(0.000216, 0.0388, 0.9620) \text{ GeV}, \\ G_{d,ij} &= 3F_{ij}, \quad (i \neq j). \end{aligned} \quad (6.14)$$

(i) Diagonal structure of RH neutrino mass matrix:

In refs. [36,37] dealing with TeV scale pseudo-Dirac RH neutrinos, a diagonal structure of F was assumed with the help of higher dimensional non-renormalizable operators in order to fit the charged fermion masses and mixings at the GUT scale. In the present model renormalizable interaction of 126_H is available the diagonal structure of F is a result of utilization of diagonal basis of down quarks as well.

This diagonal structure of f would have caused serious problem in fitting the neutrino oscillation data if we had a dominant type-II seesaw formula [8], but it causes no problem in our present model where type-II seesaw contribution to light neutrino mass matrix is severely damped out compared to inverse seesaw contribution which fits the neutrino oscillation data. Further, the resulting diagonal structure of RH neutrino mass matrix that emerges in this model has been widely used in SUSY and non-SUSY $SO(10)$ by a large number of authors, and this model creates no anomaly as there are no experimental data or constraints which are violated by this diagonal structure.

The quark mixings reflected through the CKM mixing matrix $V_{CKM} = U_L^\dagger D_L = U_L$ has been parametrized at $\mu = M_Z$ in the down-quark diagonal basis and this mixing matrix

*It is to be noted that the validity of our estimations of $0\nu\beta\beta$ decay and non-unitarity and LFV effects do not require exact equality of M_u and M_D and a relation between them within less than an order of magnitude deviation would suffice to make dominant contributions at the TeV scale. But the present models, either with G_{224D} or $SO(10)$ symmetry at the high GUT scale, give the high scale prediction $M_u^0 \sim M_D^0$ up to a good approximation.

has been extrapolated to the GUT scale resulting in $V_{CKM}^0 \equiv U_L^0$ in eq. (6.10) provided $D_L^0 = I$ which can hold even at the GUT scale if we use down quark diagonal basis. In that case $M_d(M_{GUT}) = M_d^0 = \text{diag}(m_d^0, m_s^0, m_b^0)$ which is completely determined by the respective mass eigen values determined by the bottom-up approach. Then the second mass relation of eq. (6.12) gives,

$$G_{d_{ij}} = -F_{ij}, \quad (i \neq j). \quad (6.15)$$

Now eq. (6.14) and eq. (6.15) are satisfied only if $F_{ij} = 0$, ($i \neq j$) i.e, if F is diagonal. This is also reflected directly through the eq. (6.13). In other words the diagonality of F used in earlier applications of inverse seesaw mechanism in $SO(10)$ [36,37] is a consequence of utilization of down quark and charged lepton diagonal bases and vice-versa, although through non-renormalizable Yukawa interaction. In the present model it shows that even by restricting F to its diagonal structure which eliminates at least six additional parameters which would have otherwise existed via its non-diagonal elements, the model successfully fits all the charged fermion masses and mixings including the Dirac phase of the CKM matrix at the GUT scale. Besides, as shown below, the model predicts the RH neutrino masses accessible to high energy accelerators including LHC. We have relations between the diagonal elements which, in turn, determine the diagonal matrices F and G_d completely.

$$\begin{aligned} G_{d,ii} + F_{ii} &= m_i^0, \quad (i=d,s,b), \\ G_{d,jj} - 3F_{jj} &= m_j^0, \quad (j = e, \mu, \tau). \end{aligned} \quad (6.16)$$

$$\begin{aligned} F &= \text{diag} \frac{1}{4}(m_d^0 - m_e^0, m_s^0 - m_\mu^0, m_b^0 - m_\tau^0), \\ &= \text{diag}(2.365 \times 10^{-4}, -0.0038, +0.015) \text{ GeV}, \\ G_d &= \text{diag} \frac{1}{4}(3m_d^0 + m_e^0, 3m_s^0 + m_\mu^0, 3m_b^0 + m_\tau^0), \\ &= \text{diag}(9.2645 \times 10^{-4}, 0.027224, 1.00975) \text{ GeV}, \end{aligned} \quad (6.17)$$

where we have used the RG extrapolated values of eq. (6.9). It is clear from the value of the mass matrix F in eq. (6.17) that we need as small a VEV as $v_\xi \sim 10$ MeV to carry out the fermion mass fits at the GUT scale. In the subsection 6.5.D below we show how the $SO(10)$ structure and the Higgs representations given for the symmetry breaking chain of eq. (6.1) clearly predicts a VEV $v_\xi \sim (10 - 100)$ MeV consistent with precision gauge coupling unification and the fermion mass values discussed in this subsection.

The model ansatz for CKM mixings at the GUT scale matches successfully with those given by V_{CKM}^0 of eq. (6.10) and, similarly, the model predictions for up quark masses can match with those given in eq. (6.9) provided we can identify M_u of eq. (6.12) with M_u^0 of eq. (6.11). This is done by fixing $G_u = M_u^0 - F$ leading to

$$G_u(M_{GUT}) = \begin{pmatrix} 0.00950 & 0.0379 - 0.00693i & 0.0635 - 0.1671i \\ 0.0379 + 0.00693i & 0.2637 & 2.117 + 0.000116i \\ 0.0635 + 0.1672i & 2.117 - 0.000116i & 51.4436 \end{pmatrix} \text{ GeV}. \quad (6.18)$$

Now using eq. (6.17) and eq. (6.18) in eq. (6.12) gives the Dirac neutrino mass matrix M_D at the GUT scale

$$M_D^0(M_{GUT}) = \begin{pmatrix} 0.00876 & 0.0380 - 0.00693i & 0.0635 - 0.1672i \\ 0.0380 + 0.00693i & 0.3102 & 2.118 + 0.000116i \\ 0.0635 + 0.1672i & 2.118 - 0.000116i & 51.6344 \end{pmatrix} \text{ GeV}. \quad (6.19)$$

The relation $F = f v_\xi = \text{diag}(f_1, f_2, f_3) v_\xi$ in eq.(6.15) with $v_\xi = 10 \text{ MeV}$ gives $(f_1, f_2, f_3) = (0.0236, -0.38, 1.5)^\dagger$. Then the allowed solution to RGEs for gauge coupling unification with $M_R^0 = v_R = 5 \text{ TeV}$ determines the RH neutrino masses.

$$M_{N_1} = 115 \text{ GeV}, \quad M_{N_2} = 1.785 \text{ TeV}, \quad M_{N_3} = 7.5 \text{ TeV}. \quad (6.20)$$

While the first RH neutrino is lighter than the current experimental limit on Z_R boson mass, the second one is in-between the Z_R and W_R boson mass limits, but the heaviest one is larger than the W_R mass limit. These are expected to provide interesting collider signatures at LHC and future accelerators. This hierarchy of the RH neutrino masses has been found to be consistent with lepton-number and lepton flavor violations discussed in Sec. 2, Sec. 4, and Sec. 5.

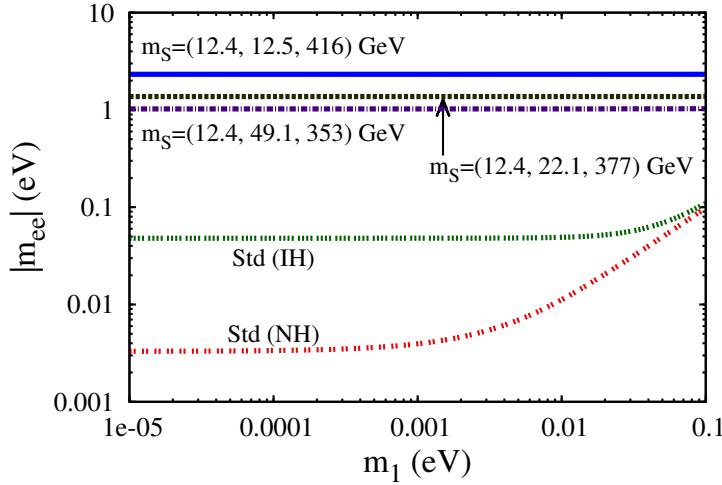


Figure 12: Estimations of effective mass parameter for $0\nu\beta\beta$ decay in the $W_L^- - W_L^-$ channel with sterile neutrino exchanges shown by top, middle, and bottom horizontal lines. The RH neutrino masses and the Dirac neutrino masses are derived from fermion mass fits and the sterile neutrino masses have been obtained through M values consistent with non-unitarity constraints as described in the text.

We estimate effective mass parameters for $0\nu\beta\beta$ decay using this predicted diagonal structure of M_N and three sets of constrained $N - S$ mixing matrix $M_i = (40, 150, 1810)$

[†]In the context of observable $n - \bar{n}$ oscillation, the value of $f_1 \sim 0.01$ and quartic coupling $\lambda \sim 1$ need the degenerate mass of diquark Higgs scalars $M_\Delta = 5 \times 10^4 \text{ GeV}$. We have checked that precision gauge coupling unification in the symmetry breaking chain remains unaltered with such mildly tuned value of diquark Higgs scalars contained in $\Delta_R(1, 3, \bar{10}) \subset 126_H$.

GeV, $M_i = (40, 200, 1720)$ GeV, and $M_i = (40, 300, 1660)$ GeV corresponding to the three sets of sterile neutrino mass eigen values $m_{S_i} = (12.4, 12.5, 416)$ GeV, $m_{S_i} = (12.5, 22.1, 377)$ GeV, and $m_{S_i} = (12.4, 49, 350)$ GeV, respectively. The estimated values of the effective mass parameters in the $W_L - W_L$ channel due to sterile neutrino exchanges have been shown in Fig.12 where the top, middle and the bottom horizontal lines represent $m_S^{\text{ee,L}} = 2.1$ eV, 1.3 eV, and 1.0 eV corresponding to the first, second and the third set, respectively. Thus the new values are found to be much more dominant compared to the standard predictions in this channel. Clearly the Heidelberg-Moscow results can be easily accommodated even for normally hierarchical or inverted hierarchical light neutrino masses.

(ii) General form of RH neutrino mass matrix:-

Although we have shown the emergence of diagonal structure of M_N from the successful fermion mass fits at the GUT scale, it is worthwhile to explore as to how this approach may also allow a general structure for the Yukawa coupling f of 126_H and hence the RH neutrino mass matrix while giving a successful fit to charged fermion masses at the GUT scale. It is clear from the above discussions that this is not possible via renormalizable interaction if the model has only a single 126_H . We introduce a second $126'_H$ with its coupling f' and all its scalar submultiplets at the GUT-Planck scale except for the component $\xi'(2, 2, 15)$ which is tuned to have its mass at the intermediate scale $M_{\xi'} \sim 10^{13}$ GeV- 10^{14} GeV. Also, as before, the VEV of the neutral component of $\Delta_R(1, 3, \bar{10}) \subset 126_H$ is used to contribute to the spontaneous breaking of $G_{2113} \rightarrow \text{SM}$, but the component $\xi(2, 2, 15)$ assumes its natural GUT scale mass without the necessity of being at the intermediate scale. All our results go through by redefining $F = f'v_{\xi'}$ and $v_{\xi'} = (10 - 100)$ MeV is realized in the same way as discussed below in Sec. 6.5 D. In this case the diagonal structure of f' gives the same successful fit to charged fermion masses and mixings at the GUT scale without affecting the allowed general structure of f and M_N . Unlike the case (i) with single 126_H discussed above, as f_1 is not constrained to be small, observable $n - \bar{n}$ oscillation is possible in this case for all diquark Higgs scalar masses $M_\Delta \sim M_C \sim 10^5 - 10^6$ GeV already permitted by RGE solutions to precision gauge coupling unification.

So far we have discussed emergence of dominant $0\nu\beta\beta$ decay rates subject to non-unitarity constraints with either a purely diagonal or nearly diagonal M_N matrix with small mixing. To test whether such results exist for a general structure, we consider a mass matrix,

$$M_N = \begin{pmatrix} 1853.67 + 320.545i & -2165.24 - 47.9844i & 2064.69 + 364.436i \\ -2165.24 - 47.9844i & 2818.92 - 210.568i & -2030.45 + 245.815i \\ 2064.69 + 364.436i & -2030.45 + 245.815i & 4610.57 - 2.67651i \end{pmatrix} \quad (6.21)$$

which has the eigen values $M_{N_i} = (115, 1750, 7500)$ GeV with the same mixings as the LH neutrinos. Using eq. (6.21), the non-unitarity constrained $N - S$ mixing matrix $M = \text{diag}(40, 150, 1810)$ GeV, and the derived value of the Dirac neutrino mass matrix from eq. (6.23) leads to the sterile neutrino mass eigen values $m_{S_i} \simeq (1, 48, 1500)$ GeV and the resulting effective mass parameters in the notations of Sec. 4- Sec. 6 are found to be

$$m_S^{\text{ee,L}} = 2.5 \text{ eV}, \quad m_N^{\text{ee,R}} = 0.02 \text{ eV}, \quad m_{\lambda,\eta}^{\text{ee,LR}} = 0.001 \text{ eV}. \quad (6.22)$$

Thus, we have shown that the dominant contribution in the $W_L - W_L$ channel due to sterile neutrino exchanges estimated using diagonal structure of M_N is also possible with its general structure. Since the form of the matrix M_N is not restricted by GUT-scale fermion mass fits, we note that the diagonal forms of M_N used in Sec.4 and in Fig.5-Fig.7 and Tables 5-6 to avoid exigency in computation belong to this class which need an additional $126'_H$ within the $SO(10)$ structure.

C. Determination of $M_D(M_{R^0})$ by top-down approach.

We use the RGEs in the top-down approach [34,37,59] for M_D in the presence of G_{224D} , G_{224} , G_{2213} , and G_{2113} to evolve $M_D(M_{GUT})$ to $M_D(M_{R^0})$ through $M_D(M_{M_P})$, $M_D(M_{M_C})$ and $M_D(M_{M_R^\pm})$ and obtain the ansatz given in eqn. (2.14) as

$$M_D = \begin{pmatrix} 0.02274 & 0.09891 - 0.01603i & 0.1462 - 0.3859i \\ 0.09891 + 0.01603i & 0.6319 & 4.884 + 0.0003034i \\ 0.1462 + 0.3859i & 4.884 - 0.0003034i & 117.8 \end{pmatrix} \text{ GeV}. \quad (6.23)$$

As can be noted from the determination of running mass eigen values at the high GUT scale of the model shown in eqn. (6.9), $b-\tau$ unification is almost perfect, although $m_\mu^0 \simeq 2m_s^0$ [‡]. In view of the fact that G_{224} symmetry with unbroken $SU(4)_C$ gauge symmetry is present in this model right from $M_C \simeq 10^6$ GeV up to the high GUT scale $M_{GUT} \sim 10^{17.5}$ GeV, the dominance of quark lepton symmetry has manifested in the fermion mass relations like $m_b^0 \simeq m_\tau^0 \simeq 1.06$ and $M_u^0 \simeq M_D^0$ at the GUT scale while making the $SU(4)_C$ -breaking effects sub-dominant. The bidoublet $\xi(2, 2, 15) \subset 126_H$ has been found to make a small contribution resulting in the mass matrix F in eq. (6.17) which plays an important role in our present model. The impressive manner in which the underlying quark-lepton symmetry manifests in exhibiting $M_u(M_{GUT}) \simeq M_D(M_{GUT})$ can be noted from the explicit forms of the two mass matrices derived at the GUT scale and shown in eq. (6.11) and eq. (6.19).

Thus, the present non-SUSY $SO(10)$ model, having predicted M_D value given in eqn. (2.14), all our discussions using TeV scale inverse see-saw mechanism including neutrinoless double beta decay, non-unitarity effects leading to lepton flavor violations, and new CP violating effects discussed in Sec.2-Sec.5, where this mass matrix has been used, are also applicable in this GUT model.

D. Determination of induced vacuum expectation value of $\xi(2, 2, 15)$

Now we show how a small induced VEV $v_\xi \sim 10$ MeV of the sub-multiplet $\xi(2, 2, 15) \subset 126_H$, which has been found to be necessary for fitting the charged fermion masses at the GUT scale, originates from the the present $SO(10)$ model. The Higgs representations needed for the symmetry breaking chain permits the following term in the Higgs potential

$$\lambda_\xi M' 210_H 126_H^\dagger 10_H \supset \lambda_\xi M' (2, 2, 15)_{126} (1, 1, 15)_{210} (2, 2, 1)_{10} \quad (6.24)$$

[‡]While running mass eigenvalues are extrapolated up to the non-SUSY $SO(10)$ unification scale in the presence of G_{2113} and G_{2213} intermediate scales [37], it has been noted that at the GUT scale $m_b^0/m_\tau^0 \simeq 1.3$, $m_\mu^0/m_s^0 \simeq 2.5$, and $m_d^0/m_e^0 \simeq 4$. Compared to refs. [36,37] where a non-renormalizable $dim. 6$ operator has also been used for fermion mass fits at the GUT scale, all the interactions used in this work are renormalizable.

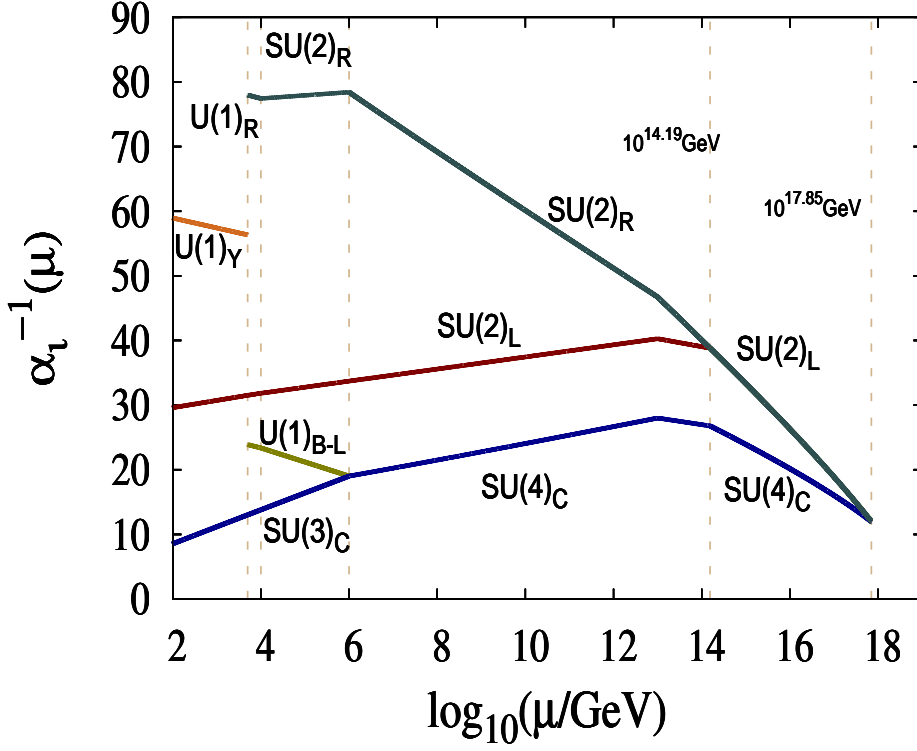


Figure 13: Same as Fig.11 but with the scalar sub-multiplet $\xi(2, 2, 15)$ under Pati-Salam group at $M_\xi = 10^{13.2}$ GeV.

where M' is a mass parameter appropriate for trilinear scalar coupling which is naturally of the order of the GUT scale $\sim \mathcal{O}(10^{18})$ GeV. For allowed solutions of the mass scales in our model, we have found $\langle(1, 1, 15)\rangle = M_C \simeq 10^6$ GeV, a criteria necessary for observable $n - \bar{n}$ oscillation and rare kaon decay. The induced v_ξ then turns out to be

$$v_\xi = \lambda_\xi M' M_C v_{ew} / M_\xi^2 \quad (6.25)$$

Using $M_C \simeq 10^6$ GeV which is required as model predictions for observable $n - \bar{n}$ oscillation and rare kaon decay, and $v_{ew} \sim 100$ GeV, we find that for $\lambda_\xi = 0.1 - 1.0$, the eq. (6.25) gives the induced VEV $v_\xi \simeq (10 - 100)$ MeV provided $M_\xi \sim 10^{13} - 10^{14}$ GeV. When $\xi(2, 2, 15)$ is made lighter than the GUT scale having such an intermediate mass, $M_\xi = 10^{13.4}$ GeV, the precision gauge coupling is found to occur as shown in Fig.13 but now with nearly two times larger GUT scale and larger GUT fine-structure constant than the minimal case. Our numerical solutions are shown in Table 11 where the Parity violating scale is close to the minimal case. It is interesting to note that the precision unification with $\xi(2, 2, 15) \subset 126_H$ at the intermediate scale is possible without upsetting low mass W_R, Z_R, M_C and other mass scale predictions of the model. The fermion mass evolutions and the emerging value of M_D remain close to the value derived in Sec.6.5.

M_ξ (GeV)	M_P (GeV)	M_{GUT} (GeV)	α_G	v_ξ (MeV)
$10^{13.2}$	$10^{14.19}$	$10^{17.83}$	0.083	25-250
$10^{13.4}$	$10^{14.19}$	$10^{17.83}$	0.076	10-100
$10^{13.5}$	$10^{14.19}$	$10^{17.83}$	0.073	7-70
$10^{13.8}$	$10^{14.20}$	$10^{17.82}$	0.068	2-16
$10^{14.0}$	$10^{14.20}$	$10^{17.81}$	0.065	1-7

Table 11: Allowed solutions in the $SO(10)$ symmetry breaking chain shown in eq. (6.1) but with the scalar component $\xi(2, 2, 15) \subset 126_H$ lighter than the GUT scale and consistent with the determination of the induced VEV $v_\xi \sim (10 - 100)$ MeV needed to fit charged fermion masses at the GUT scale. For all solutions we have fixed $M_R^0 = 5$ TeV, $M_R^+ = 10$ TeV, and $M_C = 10^6$ GeV.

The unification pattern and model predictions including GUT-scale fermion mass fit are essentially unchanged when the second $126'_H$ is introduced with its Yukawa coupling f' and the component $\xi'(2, 2, 15) \subset 126'_H$ at the intermediate scale replacing $\xi(2, 2, 15) \subset 126_H$ and the latter is assigned its natural GUT scale mass. In this case the mass scales of the model give $v_{\xi'} = (10 - 100)$ MeV. As the additional threshold contributions to $\sin^2 \theta_W$ and M_P due to the superheavy components of second $126'_H$ vanish [32], the only change that can occur is the GUT-scale threshold effects on M_{GUT} . However as the unification scale is close to the Plank scale with large proton lifetime prediction, this will not have any additional observable effects.

Thus, we have shown that the small induced VEV v_ξ or $v_{\xi'}$ needed for GUT scale fit to the charged fermion masses and prediction of M_D which is crucial for low-energy estimation of $0\nu\beta\beta$ decay rate can be easily derived from the present $SO(10)$ structure. It is possible to have a diagonal structure or a general structure for the RH neutrino mass matrix M_N for which dominant contributions to $0\nu\beta\beta$ decay, experimentally accessible LFV decays, and non-unitarity and CP-violating effects have been discussed in Sec. 4 and Sec. 5.

6.6 Suppressed induced contribution to $\nu - S$ mixing

In our model the $\nu - S$ mixing term has been chosen to be vanishingly small in eqn. (2.3). However, because of the presence of non-minimal Higgs fields including LH and RH doublets carrying $B - L = -1$, triplets carrying $B - L = -2$, two bi-doublets each with $B - L = 0$, and Parity odd singlet, it is necessary to evaluate if such a term can arise through the induced VEV of $\langle \chi_L \rangle$. We find that without taking recourse to any severe fine tuning of parameters, minimization of the scalar potential gives

$$\langle \chi_L \rangle \simeq K \frac{\langle \chi_R \rangle v}{M_P}, \quad (6.26)$$

where the ratio of parameters $K = \mathcal{O}(0.1 - .01)$ and $M_P \simeq 10^{14}$ GeV. When eqn. (6.26) is used in the corresponding correction to the light neutrino mass predictions [61], $m_\nu \simeq M_D \frac{\langle \chi_L \rangle}{\langle \chi_R \rangle}$, this gives $m_{\nu_{33}} \ll 0.001$ eV and negligible contributions to all the three light neutrino masses. With fine-tuning of parameters this contribution can be reduced further.

Thus the predictions of the model carried out using eqn. (2.3) are found to hold up to a very good approximation as the small induced contribution $\langle \chi_L \rangle$ does not affect the results substantially. Fine tuning of model parameters would result in further reduction of this contribution.

7. Summary and Conclusion

In this work we have investigated in detail the prospects of TeV scale left-right gauge theory with high scale parity restoration but originating from Pati-Salam or $SO(10)$ grand unified theory to implement extended seesaw mechanism resulting in dominant contributions to $0\nu\beta\beta$ decay and experimentally accessible LFV decays, non-unitarity and CP-violating effects, $n-\bar{n}$ oscillation, and rare kaon decays while preserving the hall-mark of such models to represent all fermion masses and mixings of three generations. Consistent with updated values of $\sin^2\theta_W(M_Z)$, $\alpha_S(M_Z)$ and $\alpha(M_Z)$ we have embedded the model successfully in non-SUSY Pati-Salam symmetry and $SO(10)$ GUT predicting low mass W_R^\pm and Z_R bosons near 1 – 10 TeV scale accessible to Large Hadron Collider (LHC) and future accelerators. We have also shown how a novel mechanism operates to realize grand unification at the GUT-Planck scale through parity conserving Pati-Salam symmetry.

The Dirac neutrino mass matrix M_D necessary to estimate lepton number and lepton flavor violating contributions, non-unitarity effects as well as leptonic CP-violation in this model has been explicitly computed using the associated renormalization group equations via bottom-up and top-down approaches, and by fitting the quark masses and mixings and the charged lepton masses of three generations at the GUT scale. The induced VEV of the Pati-Salam sub-multiplet $\xi(2, 2, 15)$ of $126_H \subset SO(10)$ needed to fit the fermion masses at the GUT scale is found to emerge naturally within the specified $SO(10)$ structure while safeguarding the precision gauge coupling unification, and values of mass scales needed for all experimentally verifiable physical processes as well as the value of the Dirac neutrino mass matrix used in our computations. The successful fermion mass fit in the model gives a diagonal structure of RH neutrino mass matrix M_N with specific eigen values accessible to accelerator searches. We have also shown how M_N is also allowed to be of general form if the model is extended to include an additional $126'_H \subset SO(10)$.

Even though the Dirac neutrino mass matrix is not subdominant but similar to the up quark mass matrix, we have shown that low mass W_R^\pm and Z_R bosons, and dominant contributions to $0\nu\beta\beta$ decay are in concordance with the neutrino oscillation data for explaining tiny masses of light neutrinos which are governed by a gauged inverse seesaw formula near the TeV scale.

In addition to the Dirac neutrino mass matrix, a major role of the sterile neutrinos, generically required in such inverse seesaw mechanism which has been found in this work is that they give the most dominant contributions to the $0\nu\beta\beta$ decay rate with effective mass parameter $\mathbf{m}_S^{\text{ee,L}} \equiv \mathbf{m}_{\text{sterile}}^{\text{ee}} \simeq (0.2 - 2.5)$ eV in the $W_L^- - W_L^-$ mediated channel depending upon the allowed range of the sterile neutrino mass eigenvalues. In addition, the next dominant contribution in the $W_L^- - W_R^-$ mediated channel due to the exchanges of light and heavy RH neutrinos and sterile neutrinos has been also computed. In the

$W_R - W_R$ channel corresponding to $M_{W_R} \simeq 3 - 5$ TeV we find the estimated value of the effective parameter to be about 2 times larger than the standard contribution for NH pattern of light neutrino masses. In addition to contributing significantly to the $0\nu\beta\beta$ rate, the quark-lepton symmetric origin of the Dirac neutrino mass matrix is also found to play a crucial role in contributing to substantial non-unitarity effects leading to enhanced lepton flavor violations and leptonic CP-violation. Even with negligible unitarity CP-violation corresponding to the leptonic Dirac phases $\delta_{\text{CP}} \simeq 0, \pi, 2\pi$, the models give non-unitarity CP-violating parameter nearly one order larger than the quark sector.

The prediction of W_R^\pm and Z_R bosons in this particular non-SUSY $SO(10)$ GUT theory is further accompanied by observable $n - \bar{n}$ oscillation with mixing time $\tau_{n-\bar{n}} \simeq (10^8 - 10^{11})$ secs as well as lepto-quark gauge boson mediated rare kaon decay with $\text{Br}(K_L \rightarrow \mu \bar{e}) \simeq (10^{-9} - 10^{-11})$ accessible to ongoing experiments. Another set of important results obtained in these models is noted to include non-unitarity effects and branching ratios for LFV decays with $\text{Br}(\tau \rightarrow e + \gamma) = 2.0 \times 10^{-14}$, $\text{Br}(\tau \rightarrow \mu + \gamma) \leq 2.8 \times 10^{-12}$, and $\text{Br}(\mu \rightarrow e + \gamma) \leq 2.5 \times 10^{-16}$ accessible to ongoing searches.

We conclude that the experimentally verifiable extended seesaw mechanism in conjunction with near TeV scale asymmetric left-right gauge theory accessible to high energy accelerators provides a rich structure of weak interaction phenomenology including light neutrino masses, neutrinoless double beta decay, non-unitarity effects, and leptonic CP-violation. These can originate from $SO(10)$ grand unified theory or high scale Pati-Salam symmetry with additional verifiable signatures like $n - \bar{n}$ oscillation and rare kaon decays. In particular, our finding on sterile neutrino mediated dominant $0\nu\beta\beta$ decay rate in the $W_L^- - W_L^-$ channel suggests that the Heidelberg-Moscow experimental data could be even consistent with light active neutrinos having NH or IH pattern of masses.

A. APPENDIX

The main goal of this section is to derive the masses and mixings for the neutrino sector in the extended seesaw mechanism which plays a prime role in determining lepton flavor violating processes like $0\nu\beta\beta$ decay rate as well as branching ratios for the lepton flavor violating decays. To start with, let us write the complete mass matrix for extended seesaw model in flavor basis $\{\nu_L, S_L, N_R^C\}$ as

$$\mathcal{M}_\nu = \begin{pmatrix} 0 & 0 & M_D \\ 0 & \mu_S & M^T \\ M_D^T & M & M_N \end{pmatrix} \quad (\text{A.1})$$

The flavor basis to mass basis transformation and the diagonalization of the above mass matrix is achieved through a unitary matrix

$$|\psi\rangle_f = \mathcal{V} |\psi\rangle_m \quad (\text{A.2})$$

$$\text{or, } \begin{pmatrix} \nu_\alpha \\ S_\beta \\ N_\gamma^C \end{pmatrix} = \begin{pmatrix} \mathcal{V}_{\alpha i}^{\nu\nu} & \mathcal{V}_{\alpha j}^{\nu S} & \mathcal{V}_{\alpha k}^{\nu N} \\ \mathcal{V}_{\beta i}^{S\nu} & \mathcal{V}_{\beta j}^{SS} & \mathcal{V}_{\beta k}^{SN} \\ \mathcal{V}_{\gamma i}^{N\nu} & \mathcal{V}_{\gamma j}^{NS} & \mathcal{V}_{\gamma k}^{NN} \end{pmatrix} \begin{pmatrix} \hat{\nu}_i \\ \hat{S}_j \\ \hat{N}_k \end{pmatrix} \quad (\text{A.3})$$

$$\text{and } \mathcal{V}^\dagger \mathcal{M}_\nu \mathcal{V}^* = \hat{\mathcal{M}}_\nu = \text{diag}(\hat{m}_{\nu_i}; \hat{m}_{S_j}; \hat{m}_{N_k}) \quad (\text{A.4})$$

where subscripts f, m denote for the flavor and mass basis, respectively. Also \mathcal{M}_ν is the mass matrix in flavor basis with α, β, γ run over three generations of light-neutrinos, sterile-neutrinos and right handed heavy-neutrinos in flavor state whereas $\hat{\mathcal{M}}_\nu$ is the diagonal mass matrix with $(i, j, k = 1, 2, 3)$ run over corresponding mass states at the sub-eV, GeV and TeV scales, respectively.

Before proceeding to diagonalize the mass matrix, the mass hierarchy $M_N \gg M > M_D, \mu_S$ as well as $\mu_S M_N < M^2$ has been assumed in our model. The method of complete diagonalization will be carried out by two step: **(1)** the full neutrino mass matrix \mathcal{M}_ν has to reduced to a block diagonalized form as \mathcal{M}_{BD} , **(2)** this block diagonal form further diagonalized to give physical masses of the neutral leptons $\hat{\mathcal{M}}_\nu$.

A.1 Block diagonalization and determination of \mathcal{M}_{BD}

We shall follow the parameterization of type given in Ref. [31] to determine the form of \mathcal{W} . In order to evaluate \mathcal{W} , let us decompose \mathcal{W} as $\mathcal{W} = \mathcal{W}_1 \mathcal{W}_2$ where \mathcal{W}_1 and \mathcal{W}_2 satisfy

$$\mathcal{W}_1^\dagger \mathcal{M}_\nu \mathcal{W}_1^* = \hat{\mathcal{M}}_{\text{BD}}, \text{ and } \mathcal{W}_2^\dagger \hat{\mathcal{M}}_{\text{BD}} \mathcal{W}_2^* = \mathcal{M}_{\text{BD}} \quad (\text{A.5})$$

where $\hat{\mathcal{M}}_{\text{BD}}$, and \mathcal{M}_{BD} are the intermediate block-diagonal, and full block-diagonal mass matrices, respectively,

$$\hat{\mathcal{M}}_{\text{BD}} = \begin{pmatrix} \mathcal{M}_{eff} & 0 \\ 0 & m_N \end{pmatrix} \quad (\text{A.6})$$

$$\text{and } \mathcal{M}_{\text{BD}} = \begin{pmatrix} m_\nu & 0 & 0 \\ 0 & m_S & 0 \\ 0 & 0 & m_N \end{pmatrix} \quad (\text{A.7})$$

A.1.1 Determination of \mathcal{W}_1

We need to first integrate out the heavy state (N_R), being heavier than other mass scales in our theory, such that up to the leading order approximation the analytic expressions for \mathcal{W}_1 is

$$\mathcal{W}_1 = \begin{pmatrix} 1 - \frac{1}{2} B^* B^T & B^* \\ -B^T & 1 - \frac{1}{2} B^T B^* \end{pmatrix}, \quad (\text{A.8})$$

where the matrix B is 6×3 dimensional and is described as

$$B^\dagger = M_N^{-1} (M_D^T, M^T) = (Z^T, Y^T) \quad (\text{A.9})$$

where, $X = M_D M^{-1}$, $Y = M M_N^{-1}$, and $Z = M_D M_N^{-1}$ so that $Z = X \cdot Y \neq Y \cdot X$ and $y = M^{-1} \mu_S$, $z = M_N^{-1} \mu_S$.

Therefore, the transformation matrix \mathcal{W}_1 can be written purely in terms of dimensionless parameters Y and Z

$$\mathcal{W}_1 = \begin{pmatrix} 1 - \frac{1}{2} Z Z^\dagger & -\frac{1}{2} Z Y^\dagger & Z \\ -\frac{1}{2} Y Z^\dagger & 1 - \frac{1}{2} Y Y^\dagger & Y \\ -Z^\dagger & -Y^\dagger & 1 - \frac{1}{2} (Z^\dagger Z + Y^\dagger Y) \end{pmatrix} \quad (\text{A.10})$$

while the light and heavy states can be now written as

$$\mathcal{M}_{eff} = \begin{pmatrix} 0 & 0 \\ 0 & \mu_S \end{pmatrix} - \begin{pmatrix} M_D M_N^{-1} M_D^T & M_D M_N^{-1} M^T \\ M M_N^{-1} M_D^T & M M_N^{-1} M^T \end{pmatrix} \quad (\text{A.11})$$

$$m_{\mathcal{N}} = M_N + .. \quad (\text{A.12})$$

A.1.2 Determination of \mathcal{W}_2

From the above discussion, it is quite clear now that the eigenstates \mathcal{N}_i are eventually decoupled from others and the remaining mass matrix \mathcal{M}_{eff} can be block diagonalized using another transformation matrix

$$\mathcal{S}^\dagger \mathcal{M}_{eff} \mathcal{S}^* = \begin{pmatrix} m_\nu & 0 \\ 0 & m_S \end{pmatrix} \quad (\text{A.13})$$

such that

$$\mathcal{W}_2 = \begin{pmatrix} \mathcal{S} & 0 \\ 0 & \mathbf{1} \end{pmatrix} \quad (\text{A.14})$$

In a simplified structure

$$-\mathcal{M}_{eff} = \begin{pmatrix} M_D Z^T & M_D Y^T \\ Y M_D^T & (M Y^T - \mu_S) \end{pmatrix} \quad (\text{A.15})$$

Under the assumption at the beginning $Z \ll Y$, and of-course $M_D \ll M$, this structure is similar to type-(I+II) seesaw. Therefore we immediately get the light neutrino masses as

$$\begin{aligned} m_\nu &= -M_D Z^T + M_D Y^T (M Y^T - \mu_S)^{-1} Y M_D^T \\ &= -M_D Z^T + M_D Z^T + M_D M \mu_S (Z Y^{-1})^T \\ &= M_D M^{-1} \mu_S (M_D M^{-1})^T \end{aligned} \quad (\text{A.16})$$

$$m_S = \mu_S - M M_N^{-1} M^T \quad (\text{A.17})$$

We see that in addition to $m_{\mathcal{N}}$ the m_S is also almost diagonal if M and M_N are taken to be diagonal. The transformation matrix S is

$$S = \begin{pmatrix} 1 - \frac{1}{2} A^* A^T & A^* \\ -A^T & 1 - \frac{1}{2} A^T A^* \end{pmatrix} \quad (\text{A.18})$$

such that

$$\begin{aligned} A^\dagger &= (M Y^T - \mu_S)^{-1} Y M_D^T \\ &\simeq (M Y^T)^{-1} Y M_D^T = X^T. \end{aligned} \quad (\text{A.19})$$

The 3×3 block diagonal mixing matrix \mathcal{W}_2 has the following form

$$\mathcal{W}_2 = \begin{pmatrix} \mathcal{S} & \mathbf{0} \\ \mathbf{0} & \mathbf{1} \end{pmatrix} = \begin{pmatrix} 1 - \frac{1}{2} X X^\dagger & X & 0 \\ -X^\dagger & 1 - \frac{1}{2} X^\dagger X & 0 \\ 0 & 0 & 1 \end{pmatrix} \quad (\text{A.20})$$

A.2 Complete diagonalization and physical neutrino masses

The block diagonal matrices m_ν , m_S and m_N can further be diagonalized to give physical masses for all neutral leptons by a unitary matrix \mathcal{U} as

$$\mathcal{U} = \begin{pmatrix} U_\nu & 0 & 0 \\ 0 & U_S & 0 \\ 0 & 0 & U_N \end{pmatrix}. \quad (\text{A.21})$$

where the unitary matrices U_ν , U_S and U_N satisfy

$$\begin{aligned} U_\nu^\dagger m_\nu U_\nu^* &= \hat{m}_\nu = \text{diag}(m_{\nu_1}, m_{\nu_2}, m_{\nu_3}), \\ U_S^\dagger m_S U_S^* &= \hat{m}_S = \text{diag}(m_{S_1}, m_{S_2}, m_{S_3}), \\ U_N^\dagger m_N U_N^* &= \hat{m}_N = \text{diag}(m_{N_1}, m_{N_2}, m_{N_3}) \end{aligned} \quad (\text{A.22})$$

With this discussion, the complete mixing matrix is

$$\begin{aligned} \mathcal{V} &= \mathcal{W} \cdot \mathcal{U} = \mathcal{W}_1 \cdot \mathcal{W}_2 \cdot \mathcal{U} \\ &= \begin{pmatrix} 1 - \frac{1}{2}ZZ^\dagger & -\frac{1}{2}ZY^\dagger & Z \\ -\frac{1}{2}YZ^\dagger & 1 - \frac{1}{2}YY^\dagger & Y \\ -Z^\dagger & -Y^\dagger & 1 - \frac{1}{2}(Z^\dagger Z + Y^\dagger Y) \end{pmatrix} \begin{pmatrix} 1 - \frac{1}{2}XX^\dagger & X & 0 \\ -X^\dagger & 1 - \frac{1}{2}X^\dagger X & 0 \\ 0 & 0 & 1 \end{pmatrix} \begin{pmatrix} U_\nu & 0 & 0 \\ 0 & U_S & 0 \\ 0 & 0 & U_N \end{pmatrix} \\ &= \begin{pmatrix} 1 - \frac{1}{2}XX^\dagger & X - \frac{1}{2}ZY^\dagger & Z \\ -X^\dagger & 1 - \frac{1}{2}(X^\dagger X + YY^\dagger) & Y - \frac{1}{2}X^\dagger Z \\ 0 & -Y^\dagger & 1 - \frac{1}{2}Y^\dagger Y \end{pmatrix} \cdot \begin{pmatrix} U_\nu & 0 & 0 \\ 0 & U_S & 0 \\ 0 & 0 & U_N \end{pmatrix} \end{aligned} \quad (\text{A.23})$$

B. One- and two-loop beta function coefficients for RG evolution of gauge couplings

Group G_I	Higgs content	\mathbf{a}_i	\mathbf{b}_{ij}
G_{1Y2L3C}	$\Phi(\frac{1}{2}, 2, 1)_{10}$	$\begin{pmatrix} 41/10 \\ -19/6 \\ -7 \end{pmatrix}$	$\begin{pmatrix} 199/50 & 27/10 & 44/5 \\ 9/10 & 35/6 & 12 \\ 11/10 & 9/2 & -26 \end{pmatrix}$
$G_{1B-L1R2L3C}$	$\Phi_1(0, \frac{1}{2}, 2, 1)_{10} \oplus \Phi_2(0, -\frac{1}{2}, 2, 1)_{10'}$ $\Delta_R(-1, 1, 1, 1)_{126} \oplus \chi_R(-\frac{1}{2}, \frac{1}{2}, 1, 1)_{16}$	$\begin{pmatrix} 37/8 \\ 57/12 \\ -3 \\ -7 \end{pmatrix}$	$\begin{pmatrix} 209/16 & 63/8 & 9/4 & 4 \\ 63/8 & 33/4 & 3 & 12 \\ 3/2 & 1 & 8 & 12 \\ 1/2 & 3/2 & 9/2 & -26 \end{pmatrix}$
$G_{1B-L2L2R3C}$	$\Phi_1(0, 2, 2, 1)_{10} \oplus \Phi_2(0, 2, 2, 1)_{10'}$ $\Delta_R(-2, 1, 3, 1)_{126} \oplus \chi_R(-1, 1, 2, 1)_{16}$ $\Sigma_R(0, 1, 3, 1)_{210}$	$\begin{pmatrix} 23/4 \\ -8/3 \\ -3/2 \\ -7 \end{pmatrix}$	$\begin{pmatrix} 253/8 & 9/2 & 171/4 & 4 \\ 3/2 & 37/3 & 6 & 12 \\ 57/4 & 6 & 263/6 & 12 \\ 1/2 & 9/2 & 9/2 & -26 \end{pmatrix}$
G_{2L2R4C}	$\Phi_1(2, 2, 1)_{10} \oplus \Phi_2(2, 2, 1)_{10'}$ $\Delta_R(1, 3, \overline{10})_{126} \oplus \chi_R(1, 2, \overline{4})_{16}$ $\Sigma_R(1, 3, 15)_{210} \oplus \sigma'(1, 1, 15)_{210}$	$\begin{pmatrix} -8/3 \\ 29/2 \\ -14/3 \end{pmatrix}$	$\begin{pmatrix} 37/3 & 6 & 45/2 \\ 6 & 1103/3 & 1275/2 \\ 9/2 & 255/2 & 288 \end{pmatrix}$
$G_{2L2R4CD}$	$\Phi_1(2, 2, 1)_{10} \oplus \Phi_2(2, 2, 1)_{10'}$ $\Delta_L(3, 1, 10)_{126} \oplus \Delta_R(1, 3, \overline{10})_{126}$ $\chi_L(2, 1, 4)_{16} \oplus \chi_R(1, 2, \overline{4})_{16}$ $\Sigma_L(3, 1, 15)_{210} \oplus \Sigma_R(1, 3, 15)_{210}$ $\sigma'(1, 1, 15)_{210}$	$\begin{pmatrix} 29/3 \\ 29/3 \\ 2/3 \end{pmatrix}$	$\begin{pmatrix} 1103/3 & 6 & 1275/2 \\ 6 & 1103/3 & 1275/2 \\ 255/2 & 255/2 & 3673/6 \end{pmatrix}$

Table 12: One and two loop beta coefficients for different gauge coupling evolutions described in text taking the second Higgs doublet at $\mu \geq 10$ TeV.

ACKNOWLEDGEMENT

Ram Lal Awasthi acknowledges hospitality at the Center of Excellence in Theoretical and Mathematical Sciences, SOA University where this work was carried out.

References

- [1] T. D. Lee and C. N. Yang, Phys. Rev. **D 104**, 254 (1956).
- [2] R. Foot, R. R. Volkas, Phys. Rev. **D 52**, 6595 (1995). Z. G. Berezhiani, R.N. Mohapatra, Phys. Rev. **D 52**, 6607 (1995).
- [3] J. C. Pati and A. Salam, Phys. Rev. **D 8**, 1240 (1973); *ibid.* **D 10**, 275 (1974).
- [4] R. N. Mohapatra and J. C. Pati, Phys. Rev. **D 11**, 2558 (1975); Phys. Rev. **D 11**, 566 (1975); G. Senjanovic and R. N. Mohapatra, Phys. Rev. **D 12**, 1502 (1975).
- [5] H. Georgi, Particles and Fields, *Proceedings of APS Division of Particles and Fields*, ed C. Carlson, (AIP, New York, 1975), p.575; H. Fritzsch, P. Minkowski, Ann. Phys. (Berlin) **93**, 193 (1975).
- [6] P. Minkowski, *Phys. Lett.* **B 67**, 421 (1977); T. Yanagida in *Workshop on Unified Theories, KEK Report 79-18*, p. 95, 1979; M. Gell-Mann, P. Ramond and R. Slansky, *Supergravity*, p. 315. Amsterdam: North Holland, 1979; S. L. Glashow, *1979 Cargese Summer Institute on Quarks and Leptons*, p. 687, New York: Plenum, 1980; R. N. Mohapatra and G. Senjanovic, Phys. Rev. Lett. **44**, 912 (1980).
- [7] J. Schechter and J. W. F. Valle, Phys. Rev. **D 22**, 2227 (1980).
- [8] M. Magg and C. Wetterich, Phys. Lett. **B 94**, 61 (1980); G. Lazaridis, Q. Shafi and C. Wetterich, Nucl. Phys. **B 181**, 287 (1981).
- [9] R. N. Mohapatra and G. Senjanovic, Phys. Rev. **D 23**, 165 (1981).
- [10] H. V. Klapdor-Kleingrothaus, A. Dietz, L. Baudis, G. Heusser, I. V. Krivosheina, S. Kolb, B. Majorovits, H. Pas et al., Eur. Phys. J. **A 12** (2001) 147-154; C. Arnaboldi et al. [CUORICINO Collaboration], Phys. Rev. **C 78**, 035502 (2008); C. E. Aalseth et al. [IGEX Collaboration], Phys. Rev. **D 65**, (2002) 092007; J. Argyriades et al. [NEMO Collaboration], Phys. Rev. **C 80**, 032501 (2009); I. Abt, M. F. Altmann, A. Bakalyarov, I. Barabanov, C. Bauer, E. Bellotti, S. T. Belyaev, L. B. Bezrukov et al., [hep-ex/0404039]; S. Schonert et al. [GERDA Collaboration], Nucl. Phys. Proc. Suppl. **145**, 242-245 (2005); C. Arnaboldi et al. [CUORE Collaboration], Nucl. Instrum. Meth. **A 518**, 775-798 (2004); H. V. Klapdor-Kleingrothaus, I. V. Krivosheina, A. Dietz, O. Chkvorets, Phys. Lett. **B 586**, 198-212 (2004); H. V. Klapdor-Kleingrothaus, I. V. Krivosheina, Mod. Phys. Lett. **A 21**, 1547-1566 (2006).
- [11] H. V. Klapdor-Kleingrothaus, A. Dietz, L. Baudis, G. Heusser, I. V. Krivosheina, S. Kolb, B. Majorovits, H. Pas et al., Eur. Phys. J. **A 12** (2001) 147-154; C. Aalseth et al., Phys. Rev. **D 65**, 092007 (2002); H. V. Klapdor-Kleingrothaus et al., Mod. Phys. Lett. **A 16**, 2409 (2001); H. V. Klapdor-Kleingrothaus, A. Dietz, and I.V. Krivosheina, Foundations of Physics **32**, 1181 (2002).
- [12] E. Majorana, N. Cim. **14** (1937) 171.
- [13] K. Abe et al., [T2K collaboration], Phys. Rev. Lett. **107**, 041801 (2011); F. P. An et al. [DAYA-BAY Collaboration], Phys. Rev. Lett. **108**, 171803 (2012); P. Adamson et al., [MINOS Collaboration], Phys. Rev. Lett. **107**, 181802 (2011); J. K. Ahn et al. [RENO Collaboration], Phys. Rev. Lett. **108**, 191802 (2012).

- [14] V. Tello, M. Nemevšek, F. Nesti, G. Senjanović, F. Vissani, Phys. Rev. Lett. **106**, 151801 (2011); Joydeep Chakraborty, H.Zeen Devi, Srubabati Goswami and Sudhanwa Patra, JHEP **1208** (2012) 008; arXiv:1204.2527 [hep-ph].
- [15] M. Nemevsek, G. Senjanovic and V. Tello, Phys. Rev. Lett. **110**, 151802 (2013); arXiv: 1211.2837 [hep-ph].
- [16] J. Barry, L. Dorame and W. Rodejohann; Eur. Phys. J. **C 72** (2012) 2023; arXiv:1203.3365 [hep-ph].
- [17] D. Chang, R. N. Mohapatra, and M. K. Parida, Phys. Rev. Lett. **52**, 1072 (1984); D. Chang, R. N. Mohapatra, and M. K. Parida, Phys. Rev. **D 30**, 1052 (1984).
- [18] D. Chang, R. N. Mohapatra, J. Gipson, R. E. Marshak, and M. K. Parida, Phys. Rev. **D 81**, 1718 (1985).
- [19] S. K. Kang and C. S. Kim, Phys. Lett. **B 646**, 248 (2007); J. Ellis, D. V. Nanopoulos and K. Olive, Phys. Lett. **B 300**, 121 (1993).
- [20] S. K. Majee, M. K. Parida, and A. Raychaudhuri, Phys. Lett. **668**, 299 (2008); M. K. Parida and A. Raychaudhuri, Phys. Rev. **D 82**, 093017 (2010); S. K. Majee, M. K. Parida, A. Raychaudhuri, and U. Sarkar, Phys. Rev. **D 75**, 075003 (2007).
- [21] G. Beall, M. Bander, and A. Soni, Phys Rev. Lett. **48** (1982) 848; A. Maiezza, M. Nemevsek, F. Nesti, and G. Senjanovic, Phys. Rev. **D 82**, 055022 (2010); arXiv: 1005.5160 [hep-ph]; D. Guadagnoli and R. N. Mohapatra, Phys.Lett. **B 694**, 386 (2011); arXiv: 1008.1074 [hep-ph]; S. Bertolini, J. O. Eeg, A. Maiezza and F. Nesti, Phys. Rev. **D 86**, 095013 (2012); arXiv:1206.0668 [hep-ph].
- [22] **ATLAS Collaboration**, G. Aad et al., Eur. Phys. J. **C 72** (2012) 2056; arXiv:1203.5420 [hep-ex]; **CMS Collaboration**, S. Chatrchyan et al., Phys. Rev. Lett. **109** (2012) 261802; arXiv:1210.2402 [hep-ex].
- [23] W. -Y. Keung and G. Senjanovic, Phys. Rev. Lett. **50**, 1427 (1983).
- [24] **Particle Data Group**, J. Beringer et al., Phys. Rev. **D 86**, 010001 (2012).
- [25] F. del Aguila, J. de Blas, and M. Perez-Victoria, JHEP **1009** (2010) 033; arXiv:1005.3998 [hep-ph].
- [26] M. Baldo-Ceolin et al. Z. Phys. **C 63** (1994) 409.
- [27] K. Arisaka et al. Phys. Rev. Lett. **70** (1993) 1049.
- [28] M. K. Parida and Sudhanwa Patra; Phys. Lett. **B 718** (2013) 1407.
- [29] R. N. Mohapatra, Phys. Rev. Lett. **56**, 561 (1986); R. N. Mohapatra, J. W. F. Valle, Phys. Rev. **D 34**, 1642 (1986).
- [30] D. Wyler, L. Wolfenstein, Nucl. Phys. **B 218**, 205 (1983); E. Witten, Nucl. Phys. **B 268**, 79 (1986).
- [31] W. Grimus and L. Lavoura, JHEP **0011**, 042 (2000); arXiv: 0008179 [hep-ph]; M. Hirsch, H. V. Klapdor-Kleingrothaus and O. Panella, Phys. Lett. **B 374**, 7 (1996), arXiv: 9602306 [hep-ph]; M. Mitra, G. Senjanovic and F. Vissani, Nucl. Phys. **B 856**, 26 (2012).
- [32] M.K. Parida and B. Purkayastha, Phys. Rev. **D 53**, 1706 (1996); N.G. Deshpande and R.J. Johnson, Phys. Rev. **D 27**, 1193 (1984); S. Dimopoulos, S. Raby, and G.L. Kane, Nucl. Phys. **B 182**, 77 (1981).

- [33] K. Nakamura *et al.* (Particle Data Group), J. Phys. **G 37**, 075021 (2010); C. Amsler *et al.* (Particle Data Group), Phys. Lett. **B 667**, 1 (2008).
- [34] C. R. Das and M. K. Parida, Eur. Phys. J. **C 20**, 121 (2001).
- [35] B. Bajc, A. Melfo, G. Senjanovic, and F. Vissani, Phys. Rev. **D 73**, 055001 (2006); H. S. Goh, R. N. Mohapatra, and S. P. Ng, Phys. Rev. **D 68**, 11508 (2003); H. S. Goh, R. N. Mohapatra, and S. Nasri, Phys. Rev. **D 70**, 075022 (2004).
- [36] P. S. B. Dev, R. N. Mohapatra, Phys. Rev. **D 81**, 013001 (2010); arXiv:0910.3924 [hep-ph].
- [37] Ram Lal Awasthi and Mina K. Parida, Phys.Rev. **D 86**, 093004 (2012); arXiv:1112.1826 [hep-ph].
- [38] E. Akhmedov, M. Lindner, E. Schnapka, and J. W. F. Valle, Phys. Rev. **D 53**, 2752 (1996); arxiv:hep-ph/9509255.
- [39] S. Antusch, J. P. Baumann, and E. Fernandez-Martinez, Nucl. Phys. **B 810**, 369 (2009); S. Antusch, M. Blennow, E. Fernandez-Martinez, and J. Lopez-Pavon, Phys. Rev. **D 80**, 033002 (2009); S. Antush, C. Biggio, E. Fernandez-Martinez, M. Belen Gavela, and J. Lopez-Pavon, J. High Energy Phys. **10** (2006) 084; D. V. Forero, S. Morisi, M. Tartola and J. W. F. Valle, J. High Energy Phys. **09** (2011) 142.
- [40] E. Fernandez-Martinez, M. B. Gavela, J. Lopez-Pavon and O. Yasuda, Phys. Lett. **B 649**, 427 (2007); K. Kanaya, Prog. Theor. Phys.,**64**,2278 (1980); J. Kersten and A. Y. Smirnov, Phys. Rev. **D 76**, 073005 (2007); M. Malinsky, T. Ohlsson, H. Zhang, Phys. Rev. **D 79**, 073009 (2009); G. Altarelli and D. Meloni, Nucl. Phys. **B 809**, 158 (2009); F. del Aguila and J. A. Aguilar-Saavedra, Phys. Lett. **B 672**, 158 (2009); F. del Aguila and J. A. Aguilar-Saavedra and J. de Blas, Acta Phys. Polon. **B 40**, 2901 (2009); arXiv:0910.2720 [hep-ph]; A. van der Schaaf, J. Phys. **G 29**, 2755 (2003); Y. Kuno, Nucl. Phys. **B**, Proc. Suppl. **149**, 376 (2005).
- [41] G. L. Fogli, E. Lisi, A. Marrone, A. Palazzo and A. M. Rotunno, Phys. Rev. **D 84**, 053007 (2011); arXiv:1106.6028 [hep-ph]; T. Schwetz, M. Tartola and J. W. F. Valle, New J. Phys. **13**, 063004 (2011); D. V. Forero, M. Tartola and J. W. F. Valle, arXiv:1205.4018[hep-ph].
- [42] R. N. Mohapatra; Phys. Rev. **D 34**, 909 (1986); M. Doi and T. Kotani, Prog. Theor. Phys. **89** (1993) 139; K. Muto, I. Blender, and H. V. Klapdor-Kleingrothaus, Z. Phys. **A 334** (1989) 177; M. Hirsch, K. Muto, T. Oda, and H. V. Klapdor-Kleingrothaus, Z. Phys. **A 347** (1994) 151; J. J. Gomez-Cadenas, J. Martin-Albo, M. Mezzetto, F. Monrabal, and M. Sorel, Riv. Nuovo Cim. **35**, 29 (2012); arXiv:1109.5515 [hep-ex]; J. Lopez-Pavon, S. Pascoli and Chan-fai Wong, arXiv:1209.5342 [hep-ph].
- [43] G. Pantis, F. Simkovic, J. Vergados, and A. Faessler, Phys. Rev. **C 53**, 695 (1996); arXiv:nucl-th/9612036 [nucl-th]; K. Muto, E. Bender, and H. Klapdor, Z. Phys. **A 334** (1989) 187; J. Suhonen and O. Civitarese, Phys. Rept. **300** (1998) 123; J. Kotila and F. Iachello, Phys. Rev. **C 85**, 034316 (2012); arXiv:1209.5722 [nucl-th].
- [44] M. Doi, T. Kotani, and E. Takasugi, Prog. Theor. Phys. Suppl. **83** (1985) 1; F. Simkovic, G. Pantis, J. Vergados, and A. Faessler, Phys. Rev. **C 60**, 055502 (1999); arXiv:hep-ph/9905509 [hep-ph]; A. Faessler, A. Meroni, S. T. Petcov, F. Simkovic, and J. Vergados, Phys. Rev. **D 83**, 113003 (2011); arXiv:1103.2434 [hep-ph].
- [45] J. Barry and W. Rodejohann, aXiv:hep-ph/1303.6324.

- [46] A. Ilakovac, A. Pilaftsis, Nucl. Phys. **B 437**, 491 (1995) [hep-ph/9403398]; F. Deppisch, J. W. F. Valle, Phys. Rev. **D 72**, 036001 (2005) [hep-ph/0406040]; C. Arina, F. Bazzocchi, N. Fornengo, J. C. Romao, J. W. F. Valle, Phys. Rev. Lett. **101**, 161802 (2008); arXiv:0806.3225 [hep-ph]; M. Malinsky, T. Ohlsson, Z. -z. Xing, H. Zhang, Phys. Lett. **B 679**, 242-248 (2009); arXiv:0905.2889 [hep-ph]; M. Hirsch, T. Kernreiter, J. C. Romao, A. Villanova del Moral, JHEP **1001** (2010) 103; arXiv:0910.2435 [hep-ph]; F. Deppisch, T. S. Kosmas, J. W. F. Valle, Nucl. Phys. **B 752**, 80 (2006); arXiv:0910.3924 [hep-ph]; S. P. Das, F. F. Deppisch, O. Kittel, J. W. F. Valle, Phys. Rev. **D 86**, 055006 (2012).
- [47] M. L. Brooks et al. [MEGA Collaboration], Phys. Rev. Lett. **83**, 1521 (1999); B. Aubert [The BABAR Collaboration], arXiv:0908.2381 [hep-ex]; Y. Kuno (PRIME Working Group), Nucl. Phys. B. Proc. Suppl. **149**, 376 (2005); For a review see F. R. Joaquim, A. Rossi, Nucl. Phys. **B 765**, 71 (2007).
- [48] T. G. Rizzo, and G. Senjanovic, Phys.Rev. **D 25**, 235 (1982); Phys.Rev. Lett. **46**, 1315 (1981); M. K. Parida and A. Raychaudhuri, Phys. Rev. **D 26**, 2364 (1982); M. K. Parida and C. C. Hazra, Phys. Lett. **B 121**, 355 (1983); M. K. Parida and C. C. Hazra, Phys. Rev. **D 40**, 3074 (1989).
- [49] S. Bertolini, L. Di Luzio and M. Malinsky, Phys. Rev. **D 80**, 015013 (2009); S. Bertolini, L. Di Luzio and M. Malinsky, Phys. Rev. **D 85**, 095014 (2012); N. G. Deshpande, E. Keith, and P. Pal, Phys. Rev. **D 46**, 2261 (1992); D. G. Lee, R. N. Mohapatra, M. K. Parida and M. Rani, Phys. Rev. **D 51**, 229 (1995).
- [50] H. Georgi, H. R. Quinn, and S. Weinberg, Phys. Rev. Lett. **33**, 451 (1974); D. R. T. Jones, Phys. Rev. **D 25**, 581 (1982).
- [51] F. del Aguila and L. Ibanez, Nucl. Phys. **B 177**, 60 (1981).
- [52] R. N. Mohapatra and G. Senjanovic, Phys. Rev. **D 27**, 1601 (1983).
- [53] B. Bajc, A. Melfo, G. Senjanovic, and F. Vissani, Phys. Rev. **D 70**, 035007 (2004); C. S. Aulakh, B. Bajc, A. Melfo, G. Senjanovic, and F. Vissani, Phys. Lett. **B 588**, 196 (2004).
- [54] R. N. Mohapatra and R. E. Marshak, Phys. Rev. Lett. **44**, 1316 (1980); [erratum- *ibid.* **44**, 1643 (1980)]. For a recent review see R. N. Mohapatra, J. Phys. **G 36**, 104006 (2009).
- [55] H. Nishino *et al.*, Phys. Rev. Lett. **102**, 141801 (2009); H. Nishino *et al.*, Phys. Rev. **D 85**, 112001 (2012).
- [56] K. S. Babu, J. C. Pati, and P. Rastogi, Phys.Lett. **B 621** (2005) 160.
- [57] M. K. Parida and P. K. Patra, Phys. Rev. Lett. **66**, 858 (1991); M. K. Parida and P. K. Patra, Phys. Rev. Lett. **68**, 754 (1992); M. K. Parida, Phys. Rev. **D 57**, 2736 (1998).
- [58] M. Blanke, A.J. Buras, K. Gemmler, and T. Heidsieck, JHEP **1203** (2012) 024; arXiv:1111.5014 [hep-ph].
- [59] T. Fukuyama and T. Kikuchi, Mod. Phys. Lett. **A 18**, 719 (2003); M. K. Parida and A. Usmani, Phys. Rev **D 54**, 3663 (1996). N. G. Deshpande and E. Keith, **D 50**, 3513 (1994).
- [60] K. S. Babu and R. N. Mohapatra, Phys. Rev. Lett. **70**, 2845 (1993).
- [61] S. M. Barr, Phys. Rev. Lett. **92**, 101601 (2004); S. M. Barr and B. Kyae, Phys. Rev. **D 71**, 075005 (2004).